

Master's Thesis 2014

Candidate: Anjana Malagalage

Title:       Near well simulation and modelling  
              of oil production from heavy oil  
              reservoirs

Telemark University College



Faculty of Technology

Kjølnes

3914 Porsgrunn

Norway

Lower Degree Programmes – M.Sc. Programmes – Ph.D. Programmes

TFver. 0.9



# Telemark University College

Faculty of Technology

M.Sc. Programme

## MASTER'S THESIS, COURSE CODE FMH606

**Student:** Anjana Tharanga Malagalage

**Thesis title:** Near well simulation and modelling of oil production from heavy oil reservoirs

**Signature:** .....

**Number of pages:** 77

**Keywords:** .AICV,ICD, Inflow control, heavy oil production, water drive, water breakthrough.  
OLGA, Rocx, Near well simulation .  
.....

**Supervisor:** Prof. Britt Halvorsen sign.: .....

**2<sup>nd</sup> Supervisor:** Dr.Eng. Vidar Mathiesen sign.: .....

**Censor:** sign.: .....

**External partner:** <name> sign.: .....

**Availability:** <Open/Secret>

**Archive approval (supervisor signature):** sign.: ..... **Date :** .....

### Abstract:

Heavy oil reservoirs cover up two third of the world's hydrocarbon reservoirs. Even though they are a vast energy reserve, heavy oil recovery is not considered economical due to its high viscous property. Generally horizontal wells are more suitable for heavy oil recovery. When the heavy oil is produced with water drive, a water breakthrough is expected in high permeable zones of the reservoir or in the heel of the well. Once water has started to be produced, heavy oil reservoirs tend to produce more water than oil.

In order to overcome this issue, inflow control devices are being used. Conventional inflow control devices are only capable in in delaying a water breakthrough. The disadvantage of ICDs is that, it cannot control the water inflow, after water breakthrough has occurred. Autonomous inflow control valve (AICV) is designed to choke the inflow as soon as the water breakthrough has occurred.

In order to evaluate the performance of AICVs in different reservoir types, OLGA-Rocx simulation system was used. As the different types of wells, fractured, heterogeneous and homogeneous reservoirs were selected. By comparing the obtained results with conventional ICDs it was found that the AICVs have a superior potential in limiting the water inflow to the base pipe (86% reduction in water accumulation compared to normal ICD in fractured reservoir). It was also observed that, AICV are more effective in heterogeneous, fractured reservoirs as it can restrict the early water breakthrough. Even in homogeneous reservoirs, AICVs have the capability in controlling the water inflow. As a result, oil production rate would also be reduced compared to the ICD system. It can be observed that when the minimum allowable flow through an AICV (when the AICV is in closed position) is increased both accumulated oil and water volumes increase.

The reopening time of the AICV valve basically depends on the viscosity and the density of the considered oil. If the viscosity is high, the time taken to reopen the valve will be increased while it will be reduced by the high density fluid. As the permeability of the of the reservoir increases, reopening time of the valve will be reduced. The reopening time also depends on the outer and inner radius of the wellbore annulus. It will increase along with the increasing outer radius and will decrease along with the increasing inner radius,

**Telemark University College accepts no responsibility for results and conclusions presented in this report.**

# Table of contents

<b>1</b>	<b>INTRODUCTION .....</b>	<b>11</b>
1.1	BACKGROUND OF THE STUDY .....	11
1.2	OBJECTIVES .....	12
<b>2</b>	<b>LITERATURE REVIEW .....</b>	<b>13</b>
2.1	HEAVY OIL PRODUCTION AND ITS CHALLENGES .....	13
2.2	INFLOW CONTROL TECHNOLOGIES .....	14
2.3	AUTONOMOUS INFLOW CONTROL VALVE (AICV) .....	15
2.3.1	<i>Theoretical background</i> .....	15
2.3.2	<i>Design and operation</i> .....	17
2.4	NEAR-WELL SIMULATIONS .....	17
<b>3</b>	<b>THEORETICAL BACKGROUND .....</b>	<b>19</b>
3.1	DARCY'S LAW .....	19
3.2	BLACK OIL – LASATER CORRELATION .....	21
3.3	COMPOSITIONAL TERMS .....	22
3.3.1	<i>GOR</i> .....	22
3.3.2	<i>GLR</i> .....	23
3.3.3	<i>Water cut</i> .....	23
<b>4</b>	<b>DEVELOPMENT OF THE OLGA-ROCX MODEL .....</b>	<b>24</b>
4.1	GRID RESOLUTION TEST AND TIME STEP ANALYSIS .....	24
4.1.1	<i>Grid resolution test</i> .....	24
4.1.2	<i>Time step analysis</i> .....	27
4.2	DEVELOPMENT OF THE RESERVOIR MODEL .....	28
4.2.1	<i>Grid</i> .....	28
4.2.2	<i>Fluid properties</i> .....	28
4.2.3	<i>Reservoir properties (permeability and porosity)</i> .....	29
4.2.4	<i>Relative permeability</i> .....	30
4.2.5	<i>Initial and boundary conditions</i> .....	30
4.2.6	<i>Simulation</i> .....	31
4.3	DEVELOPMENT OF THE WELL AND WELLBORE MODEL .....	31
4.3.1	<i>Case definition</i> .....	31
4.3.2	<i>Compositional</i> .....	31
4.3.3	<i>Flow component</i> .....	31
4.4	SIMULATED CASES .....	33
<b>5</b>	<b>DEVELOPMENT OF THE NUMERICAL MODEL .....</b>	<b>35</b>
5.1	BACKGROUND .....	35
5.2	ASSUMPTIONS .....	35
5.3	CONSERVATION OF MASS WITHIN THE WELLBORE .....	35
5.4	INFLOW TO THE WELLBORE .....	36
5.4.1	<i>When AICV is opened</i> .....	37

5.4.2	<i>When the AICV is closed</i> .....	38
5.5	OUTFLOW FROM THE WELLBORE .....	39
5.6	TIME TAKEN TO REOPEN AICV .....	40
5.6.1	<i>Equivalent wellbore tube</i> .....	40
5.6.2	<i>Time for the wellbore to be filled with gas</i> .....	40
5.6.3	<i>Time taken for the gas to exist from the wellbore</i> .....	41
5.7	CALCULATION .....	41
<b>6</b>	<b>SIMULATION RESULTS</b> .....	<b>43</b>
6.1	ANALYSIS OF THE REFERENCE CASE .....	43
6.2	COMPARING THE BASIC PERFORMANCES OF AICVS AND ICDS .....	45
6.2.1	<i>Accumulated water and oil</i> .....	45
6.2.2	<i>Oil and water flow rates</i> .....	47
6.3	EFFECTS OF DESIGN PARAMETERS OF AICV .....	49
6.3.1	<i>Pressure drop and minimum opening area</i> .....	49
6.3.2	<i>Response time</i> .....	50
6.4	FUNCTIONALITY OF THE AICVS AND ICDS IN HOMOGENEOUS RESERVOIRS .....	51
6.5	FUNCTIONALITY OF THE AICVS AND ICDS IN HETEROGENEOUS RESERVOIRS .....	53
6.6	NUMERICAL MODEL ANALYSIS .....	55
<b>7</b>	<b>DISCUSSION</b> .....	<b>57</b>
<b>8</b>	<b>CONCLUSION</b> .....	<b>58</b>
	<b>APPENDICES</b> .....	<b>59</b>
	<b>REFERENCES</b> .....	<b>77</b>

# Preface

This master thesis presents the final outcome of the research work carried out in summer 2014 at Telemark University College, Porsgrunn with InflowControl AS as an external partner. The research work along with the thesis is carried out in partial fulfillment of the Master of Science degree at Telemark University College.

The objective of this thesis work is to conduct near well simulations for oil production from heavy oil fields. In this study it was focused on inflow control technologies such as autonomous inflow control valve (AICV)

First and foremost I would like to thank both Telemark University College and InflowControl AS for granting me the opportunity to work on this interesting thesis. It is with great pleasure that I would like to thank Professor Britt Halvorsen, my thesis supervisor who guided me throughout the study. I must specially thank her for spending her valuable time in reading my draft reports and providing me with valuable advice. I would also like to thank Eng. Vidar Mathiesen from Inflow Control for guiding me with the areas where the study should be concentrated on.

I must also thank Mr. Per Morten and Mr. Øyvind Larsen for granting me permission to use the computers in Process hall in Telemark University College. I would also like to take this opportunity to thank the staff of the library and the IT department of the Telemark University College for providing me with various supports whenever needed.

Finally I would like thank my beloved wife Jayalanka, who was there with me all the time and who was encouraging me to do my best in completing this thesis work.

It would have been impossible to complete this thesis without the people whom I have mentioned and I would like to express my gratitude for all of them.

Porsgrunn, 2<sup>nd</sup> June, 2014

Anjana Malagalge

# Nomenclature

## Letters and expressions

$A$	: Area ( $m^2, cm^2$ )
$a$	: Large half axis of the drainage (m,cm,ft)
$B$	: Formation factor (-)
$f_{V,reopen}$	: Fraction of the volume of the wellbore that has to be filled with oil in order to reopen the AICV (-)
$g$	: Acceleration of gravity ( $m/s^2$ )
$h$	: Height (of the reservoir) (m,cm,ft)
$D$	:Diameter of the tube (m,cm)
$K$	: Geometrical constant (-)
$k$	: Permeability (mD,D)
$k_H$	: Horizontal permeability (mD,D)
$k_V$	: Vertical permeability (mD,D)
$I_{ani}$	: Vertical to horizontal permeability anisotropy (-)
$L$	: Length (of the well) (m,cm,ft)
$M_o$	: Molecular weight of oil (kmol/kg)
$m_{wellbore}$	: Mass of the liquid in the wellbore (kg)
$m_o/m_g$	: Mass of oil/gas (kg)
$\dot{m}_{in}$	: Inlet mass flow rate (kg/s)
$\dot{m}_{o\_in} / \dot{m}_{g\_in}$	: Inlet mass flow rate of oil/gas(kg/s)
$\dot{m}_{out}$	: Outlet mass flow rate (kg/s)
$\dot{m}_{o\_out} / \dot{m}_{g\_out}$	: Outlet mass flow rate of oil/gas(kg/s)
$\dot{Q}_l$	: Volumetric flow rate of liquid ( $cm^3/s, m^3/hr$ )
$\dot{Q}_o$	: Volumetric flow rate of oil ( $cm^3/s, m^3/hr$ )
$\dot{Q}_w$	: Volumetric flow rate of water ( $cm^3/s, m^3/hr$ )
$q$	: Volumetric flow rate ( $cm^3/s, m^3/hr$ )
$q_{g\_in} / q_{o\_in}$	: Volumetric inflow of gas/oil ( $cm^3/s, m^3/hr$ )

$q_{gi,c} / q_{oi,c}$	: Volumetric inflow of gas/oil when the AICV is closed (cm <sup>3</sup> /s, m <sup>3</sup> /hr)
$q_{g\_out,c} / q_{o\_out,c}$	: Volumetric outflow of gas/oil when the AICV is closed (cm <sup>3</sup> /s, m <sup>3</sup> /hr)
$R_s$	: Solution gas ratio (scf/STB)
$R_{sb}$	: Solution gas ratio at bubble point (scf/STB)
$r$	: Radius (m,cm,ft)
$r_w$	: Radius of the well (m,cm,ft)
$r_{we}$	: Radius of the equivalent wellbore tube (m,cm,ft)
$r_e$	: Radius of the drainage (m,cm,ft)
$r_{eH}$	: Horizontal radius of the drainage (m,cm,ft)
$T$	: Temperature (K)
$t$	: Time (s,hr)
$t_{close}$	: Time taken to completely fill the wellbore with gas (s,hr)
$t_{reopen}$	: Time taken to reopen the AICV (s,hr)
$V_{wellbore}$	: Volume of the wellbore (m <sup>3</sup> ,cm <sup>3</sup> )
$\dot{V}_{in} / \dot{V}_{out}$	: Volumetric inlet/outlet flow rate (m <sup>3</sup> /s)
$V_o / V_g$	: Volume of oil/gas (m <sup>3</sup> )
$\dot{V}_{o\_in} / \dot{V}_{g\_in}$	: Volumetric inlet flow rate of oil/gas (m <sup>3</sup> /s)
$\dot{V}_{o\_out} / \dot{V}_{g\_out}$	: Volumetric outlet flow rate of oil/gas (m <sup>3</sup> /s)
$v$	: Fluid velocity (m/s)
$y_g$	: Mole fraction of gas (-)

### Greek letters

$\gamma_g$	: Specific gravity of gas (-)
$\gamma_o$	: Specific gravity of oil (-)
$\mu$	: Viscosity (cp,Pas)
$\mu_g / \mu_o$	: Viscosity of gas/oil (cp,Pas)
$\rho$	: Density (kg/m <sup>3</sup> )
$\rho_g / \rho_o$	: Density of gas/oil (kg/m <sup>3</sup> )

## **Abbreviations**

AICV : Autonomous inflow control valve

API : American petroleum institute

GLR : Gas liquid ration

GOR : Gas oil ration

ICD : Inflow control device

ICV : Inflow control valve

psi : Pressure per square inch

PVT : Pressure volume temperture

scf : Standard cubic foot

STB : Stock tank barrel

WC : Water cut



# Overview of tables and figures

## List of Tables

Table 2-1: Oil characterisation based on API gravity and viscosity [2] .....	13
Table 3-1: Applicable units for Darcy's law .....	20
Table 3-2: Applicable data range for the Lasater model .....	22
Table 4-1: Dimensions of the reservoir .....	24
Table 4-2: Breakthrough time and accumulated oil obtained by mesh test .....	26
Table 4-3: Number of elements and their sizes in the mesh .....	28
Table 4-4: Reservoir and oil properties used for simulations .....	29
Table 4-5: Feed streams .....	29
Table 4-6: Reservoir/well model in OLGA.....	32
Table 4-7: Boundary conditions of the flow paths .....	33
Table 4-8: PID controller parameters .....	33
Table 4-9: Types of inflow control technologies .....	34
Table 5-1: Parameters for the numerical model .....	41
Table 5-2: Results obtained by numerical model calculations.....	42
Table 6-1: Accumulated oil comparison .....	46
Table 6-2: Oil production at the breakthroughs .....	48
Table 6-3: Results summary (AICV vs ICD).....	54

## List of Figures

Figure 2-1: Different types of ICDs [5] .....	14
Figure 2-2: Combination of laminar and turbulent restrictors in series [8] .....	16
Figure 2-3: Pressure drop across the combined laminar and turbulent restriction section [8].	16
Figure 2-4: Schematic view of AICV [1].....	17
Figure 3-1: Horizontal well .....	19
Figure 3-2: Drainage pattern formed around a horizontal well[13] .....	20
Figure 4-1: Location of the well in the yz-plane.....	24
Figure 4-2: Mesh of the yz plane with different discretizations in y-direction .....	25
Figure 4-3: Oil saturation profiles from mesh test .....	25

Figure 4-4: Mesh and the oil saturation profiles of meshes with 10 and 20 elements in z-direction.....	26
Figure 4-5: 3D view of the grid.....	27
Figure 4-6: Accumulated oil flow vs. time for different time steps.....	27
Figure 4-7: Vertical permeability distribution .....	30
Figure 4-8: Simplified model of a single section of the well.....	32
Figure 5-1: Gas coning.....	37
Figure 5-2: Wellbore- gas cone interface.....	37
Figure 5-3: Flow performance curve for AICV .....	39
Figure 5-4: Equivalent wellbore tube.....	40
Figure 6-1: Accumulated liquid flow of the reference case .....	43
Figure 6-2: Liquid flow rates and water cut % of the reference case.....	44
Figure 6-3: Oil saturation profile after 18 days (base case) .....	44
Figure 6-4: Oil saturation profile in the reference case after 160 days .....	45
Figure 6-5: Accumulated oil and water for comparison .....	46
Figure 6-6: Oil and water flow rate of AICV and $ICD_{ch,res}$ methods.....	47
Figure 6-7: Accumulated water and oil wrt AICV parameters .....	49
Figure 6-8: Accumulated oil and water with 2% opening AICV.....	50
Figure 6-9: Oil and water flow rates under different response-times .....	51
Figure 6-10: Accumulated water and oil profiles of homogeneous reservoir.....	52
Figure 6-11: Water and oil flow rates of homogeneous reservoirs .....	52
Figure 6-12: Accumulated water and oil profiles of heterogeneous reservoir.....	53
Figure 6-13: Water and oil flow rates of heterogeneous reservoir.....	54
Figure 6-14: Reopening time vs. oil viscosity.....	55
Figure 6-15: Reopening time vs. oil density .....	55
Figure 6-16: Reopening time vs. Permeability.....	56

# 1 Introduction

## 1.1 Background of the study

Until recently heavy crude oil production was not considered economical and little interest was shown in heavy oil field explorations. Even though heavy oil reserves are not explored as much as conventional oil fields, it is estimated that the heavy crude oil and bitumen reserves cover up 2/3 of the total crude oil reserves in the world. With the depletion of the conventional light and medium oil reserves heavy oil has a higher potential to be the solution for the future energy requirement. With the development of oil recovery technologies, and with the continuously growing oil demand and increasing oil prices have increased the economic value of heavy oil. This has resulted in a significant boost in the heavy oil recovery. Heavy oil has low mobility. So higher contact area is required within the reservoir to enhance the recoverability of oil. As horizontal wells have better contact area in the reservoirs, they are preferred over vertical wells. In order to enhance heavy oil recovery, several enhanced oil recovery (EOR) methods such as steam injection are used. For better implementation of these methods, horizontal wells are more suitable. As an example it is ideal to use horizontal wells for steam driven and steam assisted gravity drainage methods in heavy oil production.

When producing heavy oil, water/gas breakthrough can happen easily as water/gas have a higher mobility compared to heavy oil. When water/gas breakthrough occurs, oil production is reduced. In horizontal wells higher production rate can be achieved at the heel compared to the toe of the well due to frictional pressure drop in the pipe. This phenomenon which is known as toe-heel effect can lead to coning at the heel. In order to overcome the issues of water/gas breakthrough, inflow control devices (ICDs) have to be used.

Conventional ICDs are capable of delaying water/gas breakthrough but once the breakthrough occurs there is no other solution but to choke the total flow. Hence various developments have been emerged in the field of inflow control technology such as inflow control valves (ICVs). InflowControl AS is a technical company that develops products and services related to increased oil production and recovery. The company has developed an autonomous inflow control valve (AICV) which can increase the oil recovery while overcoming the problem of water/gas inflow. The objective of AICV is to minimize the water/gas inflow from the zones where the breakthrough has occurred and to allow oil production from the other zones. It is interesting to study the effectiveness of AICVs compared to conventional ICDs, under different conditions. [1]

## 1.2 Objectives

The main objective of this thesis work is to conduct near well simulations of oil production from heavy oil reservoirs with water drive. The other objective of this study is to develop a simple numerical model to express the time taken to reopen the AICV, once it is closed due to gas breakthrough. The functionality of the conventional ICDs and new AIVC technologies are studied and compared under different reservoir conditions.

## 2 Literature review

### 2.1 Heavy oil production and its challenges

Basically the major crude oil types can be categorized as light oil, heavy oil, extra heavy oil and natural bitumen. In Table 2-1 these are categorized based on their API gravity values and viscosities.

*Table 2-1: Oil characterisation based on API gravity and viscosity [2]*

<b>Oil Category</b>	<b>API gravity</b>	<b>Viscosity</b>
Light oil	$> 22^{\circ}$	$< 100$ cp
Heavy oil	$\leq 22^{\circ}$	$> 100$ cp
Extra heavy oil	$< 10^{\circ}$	
Natural bitumen		$> 10,000$ cp

Currently Canada and Venezuela are the two major countries which explore heavy oil fields and in Canada about 700,000 barrels of heavy crude oil are produced per day [3]. Recovering heavy oil is a challenging and a costly process due to its higher viscosity. In a horizontal well, the distance that the oil has to move to reach the wellbore is relatively low. Therefore horizontal wells can be considered as a better technique to recover heavy oil. With the concept of multi-lateral wells, horizontal wells can be implemented even in thick reservoirs. [4] And this technique makes sure that the maximum oil recovery is achieved in a particular reservoir, which makes it an ideal solution for heavy oil production.

The main advantage of horizontal drilling over conventional vertical drilling is its higher production rates. As a result operating costs are relatively less compared to vertical drilling. Horizontal drilling also requires less amount of wells compared to vertical drilling, to produce the same amount of oil. The major obstacle in drilling a horizontal well is the higher capital costs compared to vertical wells. Generally the cost of drilling a new horizontal well from the surface is 1.5 to 2.5 times the cost of drilling a new vertical well. The other major issue is that the overall commercial success rate of horizontal wells in USA is just 65% [4].

In addition to these disadvantages, some operational challenges have to be overcome during the oil production process. In most of the oil reservoirs oil is in contact with water and/or gas. As both water and gas have lower viscosities and hence higher mobility, water/gas breakthrough can occur during heavy oil recovery. Due to the toe-heel effect, higher oil production rate is obtained at the heel section of the well. Hence in a homogeneous reservoir, the initial water breakthrough will occur near the heel of the well.

## 2.2 Inflow control technologies

In order to control the wellbore inflow profile, inflow control devices were introduced in early 90's. The basic working principle of different ICDs is to restrict the inflow by creating an additional pressure drop. As a result wellbore pressure distribution will be adjusted causing an evenly distributed inflow profile along the horizontal well. ICDs that are being used in the oil industry can be classified as, channel type ICD and orifice/nozzle type ICD.

In channel type ICDs low fluid velocities are achieved as they move through a long channel sections. This reduces the erosion and plugging possibility of the ICD. These types of ICDs are dependent of the viscosity of the fluid. In situations where viscosity between oil and water is significantly different these ICDs are unable to maintain a uniform inflow profile when a water breakthrough occurs. In orifice/nozzle type ICDs the required pressure drop is achieved by forcing the fluid to go directly through a restriction. As a result an instant pressure drop occurs across the ICD. Therefore it is depended on the density and the velocity of the fluid and it is not depending on the viscosity of the fluid. So the orifice/nozzle type ICDs are highly prone to erosion, but not for plugging. These kinds of ICDs are suitable for applications where low sensitivity to viscosity is required.[5] Figure 2-1 shows the different types of the ICDs that are used in the industry.

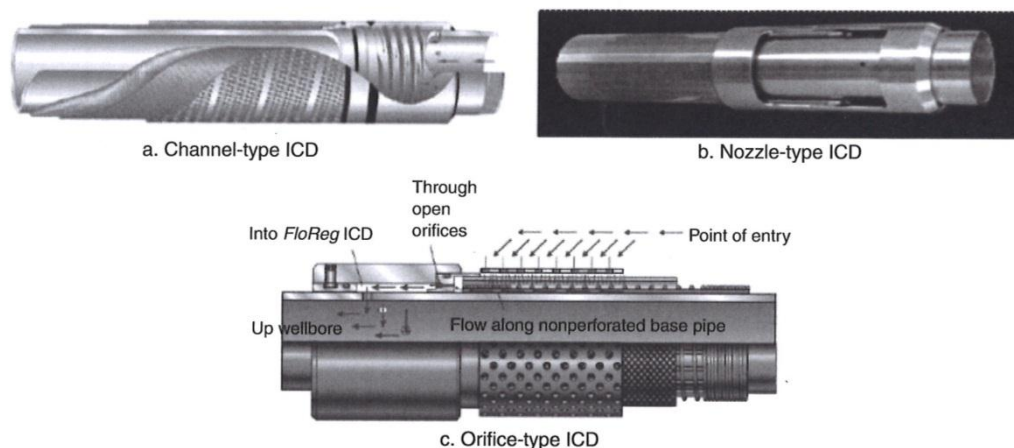


Figure 2-1: Different types of ICDs [5]

According to [5] an ICD can be effective when the pressure drop across the pipe line is relatively higher than the pressure difference between the well and the reservoir . Highly permeable reservoirs with long wells provide a favorable condition for ICDs. Furthermore if the frictional pressure drop is relatively low compared to the drawdown, ICDs can even restrict the oil flow instead of delaying water inflow. If the permeability distribution can be understood, ICDs can be effectively used in heterogeneous reservoirs to delay the water breakthrough. It can be concluded that the ICDs are not a universal solution for water breakthrough problem. It is essential to have a good understanding of the long term behaviour of the well and its characteristics before implementing inflow control technologies.

ICD is a fixed instrument. Once it is installed in a particular application, neither its location nor its relationship between the pressure drop and the flow rate can be changed. That is the reason for ICDs not being able to prevent water/gas inflow. Another type of inflow control technology that has been developed in order to overcome this drawback is the inflow control valve (ICV). These are sliding-sleeve valves installed along the pipeline. By using a downhole monitoring system, ICVs can be operated by a controlling system which is located at the surface. ICVs are considered as active controllers while ICDs are considered as passive controllers. When the information about the reservoir is not available, ICVs have the potential to deliver higher recovery compared to ICDs. ICVs exhibit a flexibility to operate according to the changing properties in the reservoir. ICVs are more expensive than ICDs and ICDs are more simple and reliable compared to ICVs as they have no moving parts, therefore ICDs have a less installation risks.[5, 6]

The newest inflow control technique is to use autonomous instruments which can adjust their functionality autonomously according to the dynamics of the wellbore. Autonomous inflow control devices are being developed by companies such as Halliburton and Statoil. Statoil has produced a rate controlled production (RCP) valve which chokes the low viscous flows while permitting high viscous flow to go through the valve. It operates autonomously based on the Bernoulli Effect. Studies conducted on RCP valve show that it can enhance the accumulated oil production by 20% compared to traditional ICD completion [7].

## 2.3 Autonomous inflow control valve (AICV)

AICV is a completely self-operating device, which has been designed by combining the features of both AICD and ICV. Its autonomous functionality is achieved by designing it in a way to distinguish between fluids based on their density and viscosity. Fundamental theory behind the operation of AICV is the difference between the pressure drop in a laminar flow restrictor and a turbulent flow restrictor.

### 2.3.1 Theoretical background

Pressure drop within the laminar flow restrictor is analogous to a pipe segment and the pressure drop is given by the equation (2.1).

$$\Delta P = \frac{32 \cdot \mu \cdot v \cdot L}{D^2} \quad (2.1)$$

In a turbulent restrictor, pressure drop can be related with a thin orifice plate and the relevant pressure drop is given by equation (2.2).

$$\Delta P = K \cdot \frac{1}{2} \cdot \rho \cdot v^2 \quad (2.2)$$

According to these relations, pressure drop within a laminar flow restrictor depends on the viscosity and the velocity of the fluid. In a turbulent restrictor, the pressure drop depends on the density and the velocity of the fluid. AICV consists of a component which can be considered as a laminar flow restrictor and a turbulent flow restrictor connected in series which is shown in Figure 2-2. Laminar flow restrictor is represented by section 1 while the turbulent restrictor is represented by section 2. As the fluid enters the inlet (section 7) it has to go through both flow restrictors. Depending on the fluid characteristics, pressure in chamber B will vary. Pressure in chamber B is used to control the valve. When a high viscous fluid (oil) goes through the laminar flow restrictor, a higher pressure drop will occur according to (2.1). When a low viscous fluid (water) passes through the laminar flow restrictor, it will result in a relatively low pressure drop.

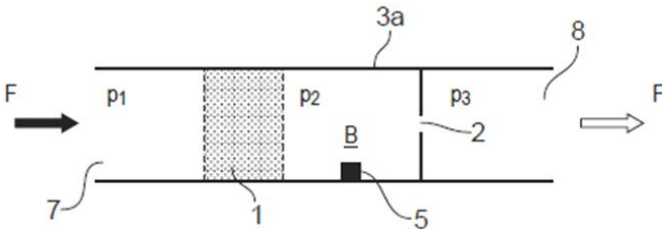


Figure 2-2: Combination of laminar and turbulent restrictors in series [8]

Pressure variation for oil, water and gas through the laminar and turbulent restricting section is shown in Figure 2-3.

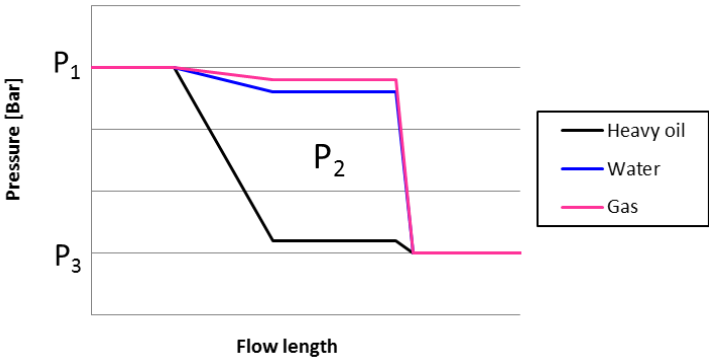


Figure 2-3: Pressure drop across the combined laminar and turbulent restriction section [8]

AICV is designed to be opened when the pressure in chamber B ( $P_2$ ) is relatively lower than the pressure in the inlet section ( $P_1$ ). That is when a higher pressure drop occurs via the laminar flow restrictor at section 1, AICV will be kept open. When oil flows through the restrictors, relatively higher pressure drop occurs through section 1 due to its high viscosity. As a result the pressure in chamber B will be lowered and the valve will be kept open. When a low viscous fluid (gas/water) flows through the restrictors relatively lower pressure drop will occur through the laminar restrictor. This will result in a relatively higher pressure in chamber B, which will force the valve to be closed.



## 2.3.2 Design and operation

In an AICV a pilot flow which is less than 1% of the total flow is allowed to pass through the laminar and turbulent flow restrictors to generate the pressure difference that is required to control the main flow by controlling the valve functionality. In Figure 2-4 it is shown how these two flow restrictors are connected within the valve.

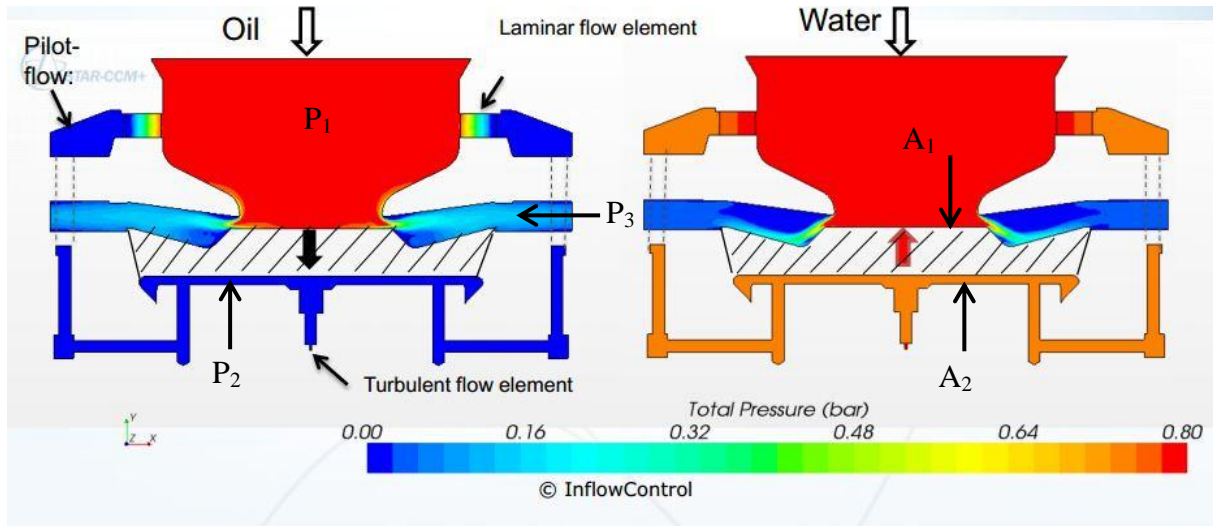


Figure 2-4: Schematic view of AICV [1]

As the flow enters the inlet section of the valve, the pilot flow will pass through the laminar and turbulent flow restrictors. The force acting on the upper part of the piston ( $F_1$ ) is in the downward direction and it is given by  $(P_1 - P_3) \cdot A_1$  where  $P$  denotes for pressure and  $A$  denotes for the cross sectional area. The upward force acting on the lower part of the piston ( $F_2$ ) is given by  $(P_2 - P_3) \cdot A_2$ . When the net force ( $F_1 - F_2$ ) is positive, the valve will be in open position allowing the fluid to enter the base pipeline. As shown in Figure 2-4 when oil enters the valve, it will have a lower  $P_2$  due to higher pressure drop through the laminar flow restrictor. As a result the net force acting on the piston will be positive and significantly higher than the net force achieved when water is passing through the valve. Whatever the type of fluid that passes through the valve,  $P_2$  will always be less than  $P_1$ . Hence  $A_2$  has to be larger than  $A_1$  and the optimum ratio between  $A_1$  and  $A_2$  depends on the properties of the considered fluids [8].

## 2.4 Near-well simulations

Conventional reservoir and well simulators are not sophisticated enough to simulate phenomena like coning where dynamic wellbore-reservoir interactions play a major role. A steady state inflow performance relationship (IPR) is being used in conventional dynamic well flow models. This method does not account for the dynamics in the near well zone. At

the same time steady state lift curves are used by the conventional reservoir models to represent a tubing performance relationship (TPR) which again does not consider the flow dynamics in the wellbore. This drawback can be overcome by combining a transient wellbore flow model with a near-well reservoir model. [9]

OLGA-ROCX combination is one of the leading commercially available transient wellbore-reservoir flow models. OLGA is a transient wellbore flow model while Rocx is a near-well flow model. Rocx is connected to OLGA as plug-in. The coupling is done via an implicit scheme where both read the same PVT file. The wellbore pressure is sent to Rocx by OLGA, and Rocx calculates the fractional flow rate of each phase [10].

In addition to OLGA-Rocx, Eclipse<sup>TM</sup> and NETools<sup>TM</sup> are two other commercially available simulators which can be used to simulate phenomena such as coning. Eclipse<sup>TM</sup> is a reservoir simulator and in order to simulate ICDs it divides the wellbore into number of segments. Parts of the tube, annulus and intermediate component such as ICDs are represented by these individual segments. In [7] Eclipse reservoir simulator was used to compare the functionality of RCP valves with conventional ICDs. NETools<sup>TM</sup> is a wellbore simulator. The model can simulate different types of ICDs in different reservoir conditions. But it is not coupled with a reservoir simulator and hence data has to be imported from a reservoir simulator. NETools<sup>TM</sup> is used to conduct simulations in [11] in order to study the functionality of ICDs.

In [12] OLGA-ROCX has been used to study the application of ICD in heavy oil production and it was successfully implemented for oil with viscosity of 100cp and 500cp. A thorough analysis between AICVs and ICDs were done in [8] using OLGA-ROCX under different conditions in the well. As successful simulations have been conducted with regarding AICV and ICD, OLGA-ROCX was used to conduct the simulations in this thesis work.

### 3 Theoretical background

#### 3.1 Darcy's law

Darcy's law is used to describe the flow through a porous medium such as oil reservoirs. The general mathematical formula for Darcy's law can be expressed as,

$$q = -\frac{k}{\mu} \nabla P \tag{3.1}$$

A horizontal oil well can be represented by a cylindrical tube. As shown in Figure 3-1 reservoir can be represented by an outer annulus which has the same axis of the well. Hence the flow from the reservoir into the well can be considered as a radial flow.

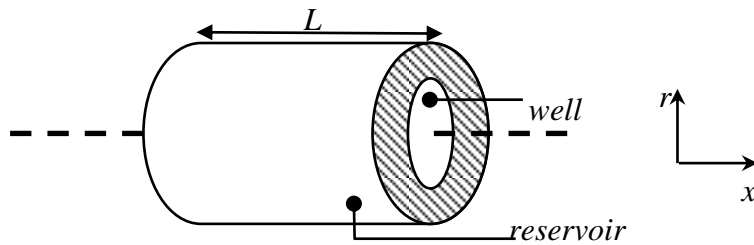


Figure 3-1: Horizontal well

For radial flow, Darcy's law can be expressed by using cylindrical coordinates as in (3.2),

$$q = \frac{kA}{\mu} \frac{dP}{dr} \tag{3.2}$$

Where  $A$  is the radial surface area at a distance of radius  $r$ , and it is given by (3.3)

$$A = 2\pi rL \tag{3.3}$$

Units that are applied in (3.2) and (3.3), are listed in Table 3-1. However SI units can also be applied for these equations.

Table 3-1: Applicable units for Darcy's law

Parameter	Units
Length of the reservoir (L)	cm
Radius (r)	cm
Viscosity( $\mu$ )	cp
Absolute permeability(k)	Da
Pressure difference( $\Delta P$ )	atm
Volumetric flow (q)	cm <sup>3</sup> /s

Pressure difference between the reservoir and the well, acts as the driving force for the radial flow in the reservoir. According to (3.2) flow will increase when the absolute permeability of the reservoir increases and the flow will be reduced if the viscosity of the considered fluid is increased.

This simple relationship is derived for a homogeneous reservoir where permeability ( $k$ ) is constant. In a reservoir, vertical permeability ( $k_v$ ) differs from horizontal permeability ( $k_H$ ). Due to the difference between these permeabilities, an ellipsoidal drainage is formed around the well and it is shown in Figure 3-2.

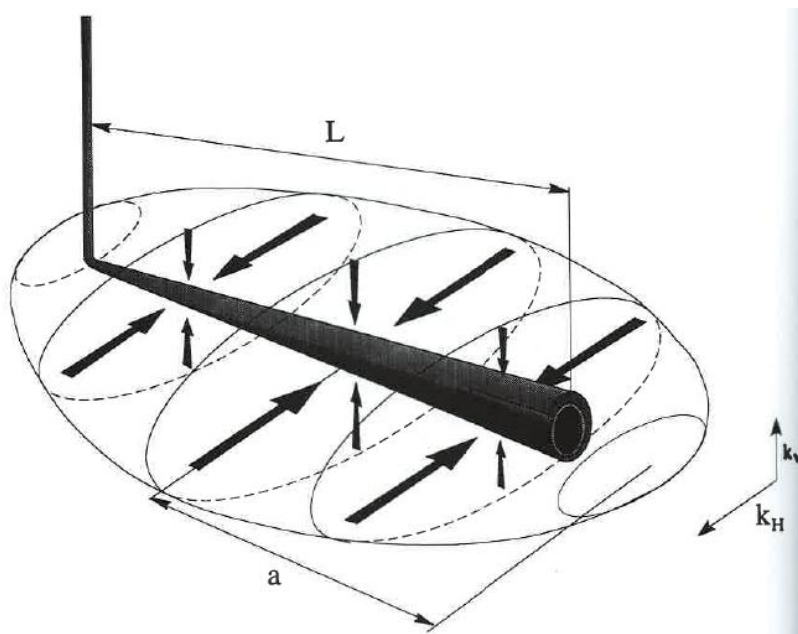


Figure 3-2: Drainage pattern formed around a horizontal well[13]

To account for this phenomenon, modified form of Darcy's law can be presented as in (3.4) [13]

$$q = \frac{k_H h \Delta P}{141.2 B \mu \left( \ln \left\{ \frac{\left[ a + \sqrt{a^2 - (L/2)^2} \right]}{L/2} \right\} + \left( \frac{I_{ani} h}{L} \right) \ln \left[ \frac{I_{ani} h}{r_w (I_{ani} + 1)} \right] \right)} \quad (3.4)$$

Where  $I_{ani}$  represents the vertical to horizontal permeability anisotropy and it is represented by (3.5),

$$I_{ani} = \sqrt{\frac{k_H}{k_V}} \quad (3.5)$$

As shown in Figure 3-2,  $a$  is the large half axis of the drainage and it can be expressed by (3.6),

$$a = \frac{L}{2} \left\{ 0.5 + \left[ 0.25 + \left( \frac{r_{eH}}{L/2} \right)^4 \right]^{0.5} \right\}^{0.5} \quad \text{for } \frac{L}{2} < 0.9 r_{eH} \quad (3.6)$$

For the equation from (3.4) to (3.6), viscosity has to be expressed in millidarcy [mD] and for other terms imperial units (British units) have to be used. Then the flow rate will be calculated in stock tank barrels per day [STB/d].[13]

## 3.2 Black oil – Lasater correlation

When conducting reservoir simulations, PVT (Pressure Volume Temperature) relations of the considered fluid are essential. These relations have to be derived by conducting experimental work. As it is difficult to establish PVT relations for all the fluids, several correlations have been used to estimate the PVT relations. Such mathematical correlations are known as black oil models, and for oil having  $17.9^0 < \text{API} < 51.1^0$  (heavy oil) Lasater model can be applied. The basic correlations in the Lasater model are as follows, [14]

### Bubble point pressure

$$P_b = \frac{0.2268 \cdot 10^{(4.258 y_g)} (T + 459.67)}{\gamma_g} \quad \text{for } (y_g \leq 0.7) \quad (3.7)$$

$$P_b = \frac{(8.26 y_g^{3.56} + 1.95)(T + 459.67)}{\gamma_g} \quad \text{for } (y_g > 0.7) \quad (3.8)$$

### Separator gas mole fraction

$$y_g = \frac{R_{sb} / 379.3}{R_{sb} / 379.3 + 350 y_g / M_o} \quad (3.9)$$

### Effective oil molecular weight

$$M_o = 630 - 10 \cdot \gamma_{API} \text{ for } (API \leq 40) \quad (3.10)$$

$$M_o = 73,110 \cdot \gamma_{API}^{-1.562} \text{ for } (API > 40) \quad (3.11)$$

### Solution gas ratio

$$R_s = \frac{137,755 \cdot \gamma_o \cdot y_g}{M_o(1 - y_g)} \quad (3.12)$$

### Bubble point pressure factor

$$P_f = \frac{P_b \gamma_g}{(T + 459.67)} \quad (3.13)$$

### Seperation gas mole fraction

$$y_g = \frac{\ln\left(\frac{P_f}{0.2268}\right)}{4.258} \text{ for } (P_f \leq 5) \quad (3.14)$$

$$y_g = \left(\frac{P_f - 1.95}{8.26}\right)^{0.2809} \text{ for } (P_f > 5) \quad (3.15)$$

In Table 3-2, the applicable data range for the Lasater model is given

*Table 3-2: Applicable data range for the Lasater model*

Conditions	Units
$48 < P_b < 5780$	psia
$82 < T < 272$	$^{\circ}\text{F}$
$3 < R_{sb} < 2905$	Scf/STB
$0.574 < \gamma_g < 1.223$	(air = 1)

## 3.3 Compositional terms

### 3.3.1 GOR

Gas - oil ratio (GOR) is the ratio between volumetric gas flow and volumetric oil flow. This represents how much gas is associated with oil flow. Mathematically it can be expressed as in (3.16).[15]

$$GOR \left[ \frac{sm^3}{sm^3} \right] = \frac{\dot{Q}_g}{\dot{Q}_o} \quad (3.16)$$

### 3.3.2 GLR

Gas - liquid ratio (GLR) is the ratio between volumetric gas flow and total volumetric liquid flow. This represents much gas is there in the total flow from the well. GLR can be expressed according to (3.17). [15]

$$GLR = \frac{\dot{Q}_g}{\dot{Q}_l} = \frac{\dot{Q}_g}{\dot{Q}_w + \dot{Q}_o} \quad (3.17)$$

### 3.3.3 Water cut

Water cut (WC) is the ratio between the volumetric water flow and volumetric oil flow. This represents how much water is associated with the oil flow. Generally it is expressed as a percentage according to (3.18).[15]

$$WC\% = \frac{\dot{Q}_w}{\dot{Q}_w + \dot{Q}_l} 100\% \quad (3.18)$$

# 4 Development of the OLGA-Rocx model

In order to study and compare the performances of AICVs and ICDs in heavy oil production process, a model was developed using OLGA-Rocx. The methodology adopted in developing this model is described along with the applied techniques and reservoir and fluid properties.

## 4.1 Grid resolution test and time step analysis

Computer simulations need to be accurate as well as time efficient. A finer mesh and smaller time steps will give accurate results but will consume significant amount of simulation time and computational resources. Hence the first step that had to be followed in developing the model was to conduct a mesh test and a time step analysis to choose a suitable time step and a mesh for the particular application.

### 4.1.1 Grid resolution test

Dimensions of the considered reservoir are mentioned in Table 4-1. Generally an AICV is installed per a zone having a length of 12.4 m of the well. It is difficult to simulate a real well with several AICVs as it requires significant amount of computational resources. Hence an equivalent AICV was selected to represent 8 AICVs. Therefore the length of the well zone containing the equivalent AICV is 99.2 m.

Table 4-1: Dimensions of the reservoir

Length of the reservoir (x)	992 m
Height of the reservoir (z)	20 m
width of the reservoir (y)	80 m

The horizontal well that is being simulated is located parallel to the x-direction. Location of the well in yz-plane is shown in Figure 4-1.

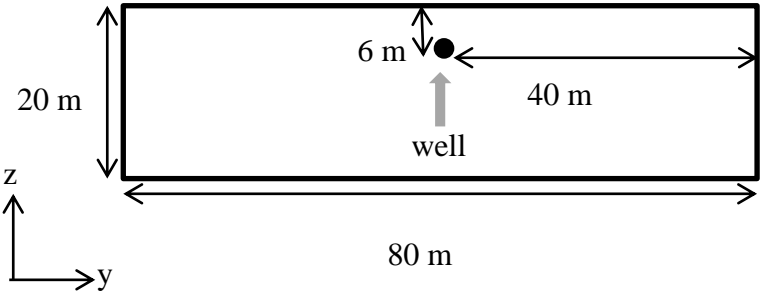


Figure 4-1: Location of the well in the yz-plane



As the simulations are conducted with water drive, it is expected to have a water-coning from the bottom boundary of the reservoir towards the well (in z-direction). Therefore a finer mesh is required close to the well. A mesh converging towards the center can be applied in y-direction to have a finer mesh around the well while reducing the total number of elements. In z-direction a uniform mesh would be acceptable.

Three parallel simulations were conducted for a reservoir segment with a length of 99.2 m having only one element in the x-direction and having 20 uniform elements in z-direction. For the test, three different meshes were developed having 59, 39 and 29 elements in the y-direction. The three meshes are shown in Figure 4-2.

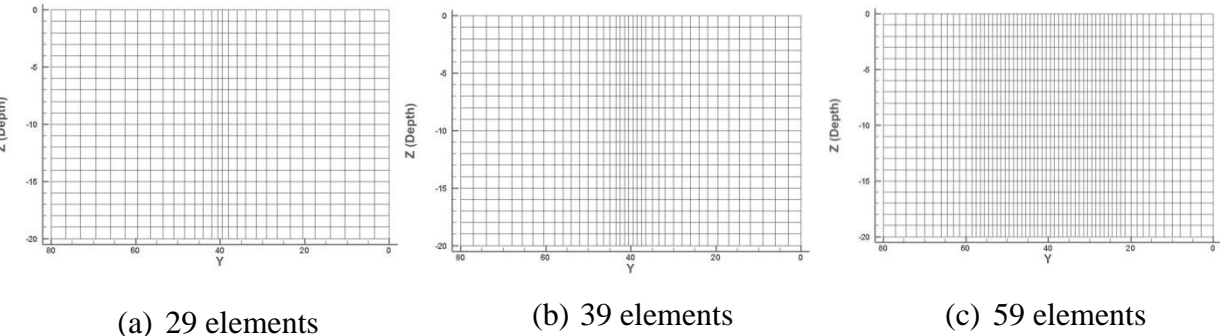


Figure 4-2: Mesh of the yz plane with different discretizations in y-direction

For this particular mesh test, permeability in the horizontal directions (x and y) was taken as 4000 mD and the permeability in the vertical direction (z) was taken as 400 mD. Minimum time step used for the simulations was 0.1 s. To analyze the effect of the element size in y direction, oil saturation profile at water breakthrough is studied. Time taken for the breakthrough and the accumulated oil and liquid flow rates are also important factors which have to be considered when selecting the suitable grid. The oil saturation profiles in the yz plane of the considered meshes are shown in Figure 4-3.

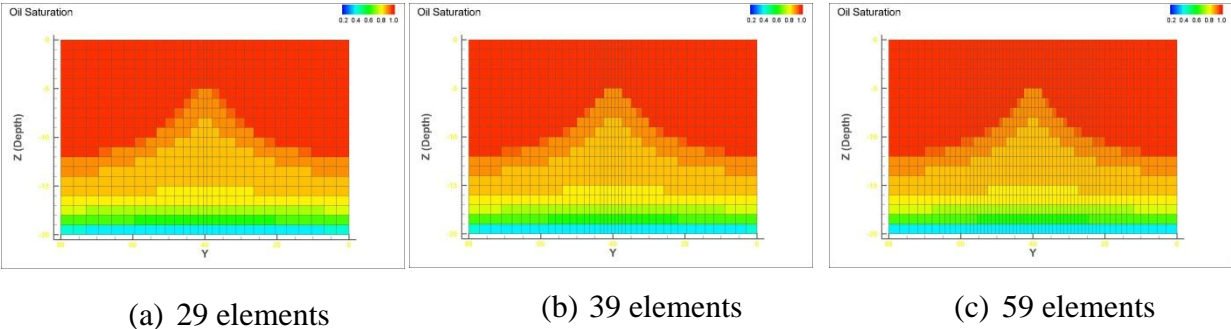


Figure 4-3: Oil saturation profiles from mesh test

By analyzing the oil saturation profiles in Figure 4-3 it can be concluded that there is no significant difference between all the profiles. It is desired to have less amount of element to reduce the computational resources and also to obtain fast results. Therefore mesh with 29 element in y-direction can be considered as a suitable mesh for the study. In order to check

whether the number of elements in z-direction can also be reduced, similar simulation was conducted having a mesh with 10 elements in the z-direction. A diagram of the mesh and the obtained oil saturation profile is shown in Figure 4-4.

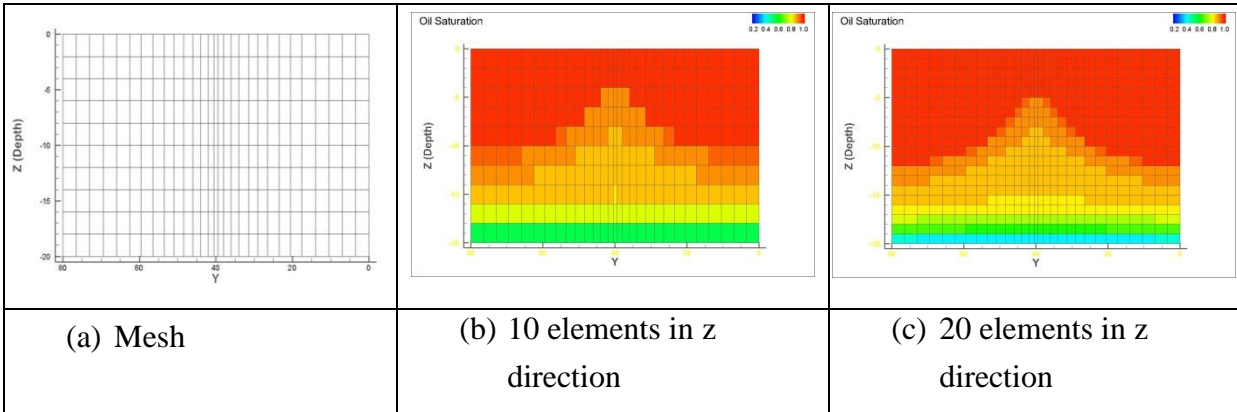


Figure 4-4: Mesh and the oil saturation profiles of meshes with 10 and 20 elements in z-direction

By comparing the Figure 4-4 (c) and (b) shape of the cone is more accurately described by the mesh having higher number elements in the z direction. Having a less number of elements in z-direction still provides a decent coning profile which is enough to understand the flow behaviour in the reservoir. In a study conducted to analyse the effect of inflow control technologies in oil production, basic description of the fluid distribution in the reservoir is adequate to decide whether the results are acceptable.

As the results obtained by using the mesh with 59 elements in y-direction, must be the most accurate data, results of two meshes with 10 and 20 elements in z-direction can be compared with it. Table 4-2 shows the time taken for water breakthrough and the accumulated oil flow at the time of the breakthrough.

Table 4-2: Breakthrough time and accumulated oil obtained by mesh test

Case	Description	Time when breakthrough occurs (days)	Accumulated oil flow when the break through occurs (m <sup>3</sup> )
Case 1	59 y with 20 z	49. 58	2737.85
Case 2	29 y with 20 z	49.58	2737.85
Case 3	29 y with 10 z	49.54	2736.64

It can be seen that the deviation between case 3 and case 1 is insignificant. Therefore it was concluded that the mesh with 29 y-direction elements and 10 z-direction elements is the suitable mesh for conducting simulations in this study.

Final mesh having 10 x-directional elements which have a length of 99.2m each, is shown in Figure 4-5

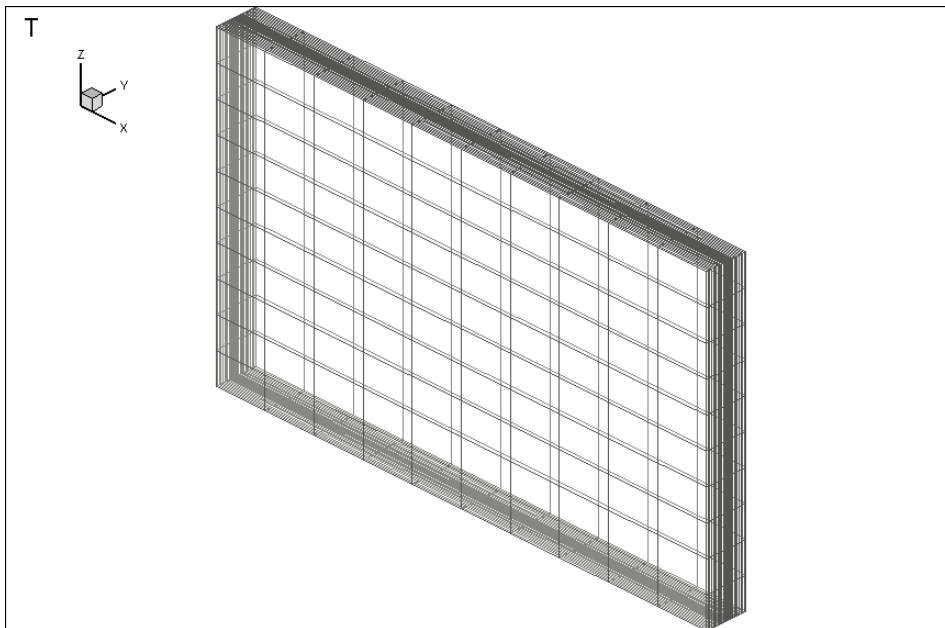


Figure 4-5: 3D view of the grid

## 4.1.2 Time step analysis

Once a suitable mesh is selected, a suitable minimum time step has to be decided to conduct the simulation in a time efficient manner. The same simulation was conducted with using 1s, 10s, 100s, 200s and 300s as the minimum time step in OLGA. The accumulated oil profiles under these time steps are shown in Figure 4-6.

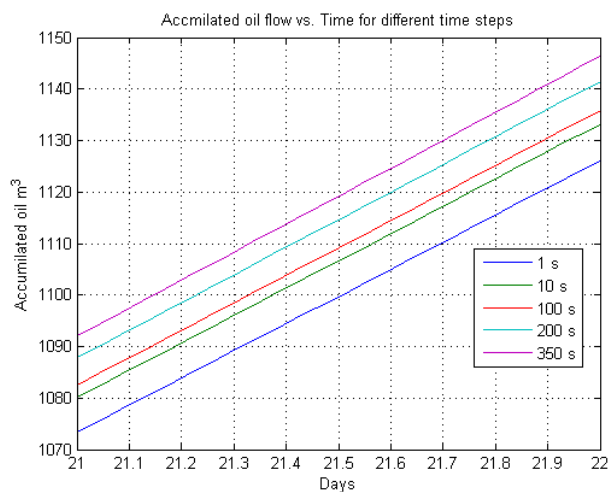


Figure 4-6: Accumulated oil flow vs. time for different time steps

It is assumed that the lowest time step will provide the most accurate results and also will require the longest computational time. Hence simulation having 1s as the minimum time step is taken as the base case. According to Figure 4-6 it can be seen that, when the minimum time step is increased the results tend to deviate from the base case. After 21.5 days case with 350s as has been deviated by 2% from the base case while 100s case has deviated only by 1%. The associated error difference between the cases of 10s and 100s is lower considering 10 times

difference between the two time steps. When two identical cases are used to simulate and compare the effect of one parameter, error associated with the time step becomes less significant as long as the same time step is used in both cases. Therefore 100s was taken as the minimum time step for conducting the simulations in this study.

## 4.2 Development of the reservoir model

Reservoir properties such as reservoir dimensions, permeability, relative permeability, porosity, and fluid properties were used to generate the reservoir model in Rocx. The boundary conditions and initial values were also included there.

### 4.2.1 Grid

As mentioned in section 3.1, dimension of the reservoir is given in Table 4-1. The mesh was developed within 3-D Cartesian coordinate system (rectangular grid). Number of elements in each direction and their respective lengths are tabulated in Table 4-3. Direction vector of gravity was set as 1 in the direction of z.

Table 4-3: Number of elements and their sizes in the mesh

Direction	Number of elements	Size of the elements (m)
X	10	99.2 (constant)
Y	29	3.5,3.5,3.5,3.5,3.5,3.3,3.3,2.5,2.5,2.5,2.2,1.5, 1,1.5,2,2,2.5,2.5,2.5,3,3,3,3.5,3.5,3.5,3.5
Z	10	2 (constant)

### 4.2.2 Fluid properties

Under the fluid properties, black-oil model was selected over PVT table as black-oil model is a simplified model which can be used for systems which are not highly volatile [16]. The basic properties of heavy oil and the conditions of the reservoir that were considered in the simulations are given in Table 4-4.

*Table 4-4: Reservoir and oil properties used for simulations*

Oil viscosity	150 cp (at 130 bar, 100 <sup>0</sup> C)
Oil specific gravity	0.92
Gas specific gravity	0.64
GOR (Sm <sup>3</sup> /Sm <sup>3</sup> )	50

As the API gravity of oil is less than 22<sup>0</sup>, LASATER model was chosen as the GOR model and mass fraction was selected as the fraction type. Oil viscosity tuning was also enabled for the simulations.

For the black-oil model, oil, gas and water components are defined according to Table 4-4. For simulating a case with water drive two feed steam have to be defined for oil and water. The respective feed streams are defined in Rocx as tabulated in Table 4-5.

*Table 4-5: Feed streams*

Stream	Fraction type	Fraction	Watercut
Oil	GOR	50	0.0001
Water	GLR	0.0001	0.99

### 4.2.3 Reservoir properties (permeability and porosity)

For all the simulations, porosity of the reservoir was considered as 0.3 which is constant throughout the reservoir. Three types of reservoirs based on their permeability profiles were considered in this study. Those three types are,

- Heterogeneous reservoir with a highly permeable zone (fractured reservoir)
- Heterogeneous reservoir with a relatively high permeable zone and with a relatively lower permeable zone.
- Homogeneous reservoir

In each cell of all reservoirs, permeability in horizontal directions ( $k_H$ ) (x and y directions) was considered 10 times higher than the vertical permeability ( $k_V$ ) (z-direction) of that particular cell. Vertical permeability profiles of the three reservoirs are shown in Figure 4-7.

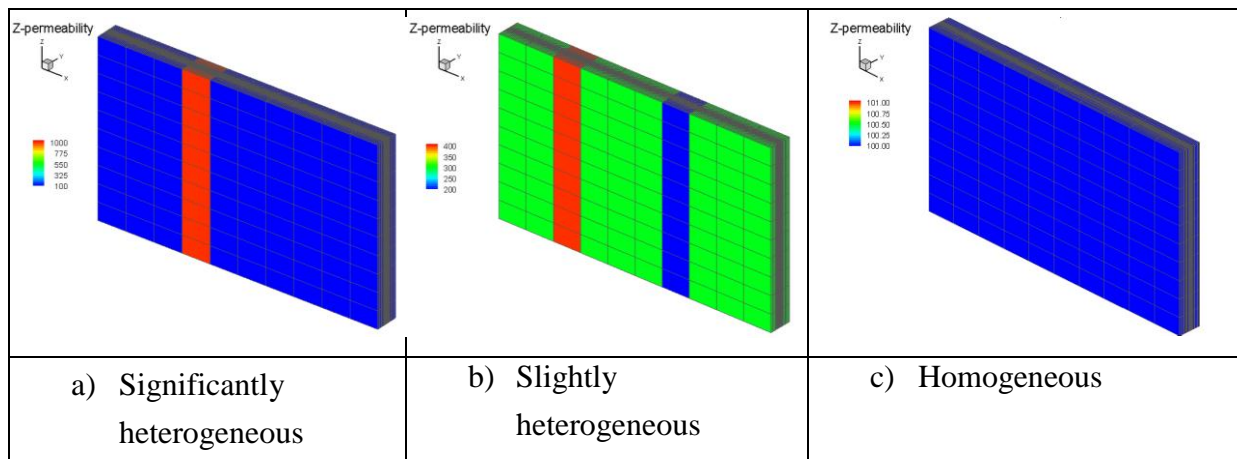


Figure 4-7: Vertical permeability distribution

## 4.2.4 Relative permeability

For the relative permeable data, default values provided by Rocx were used. These relative permeability data are presented in Appendix 2: Reservoir model in Rocx

## 4.2.5 Initial and boundary conditions

### 4.2.5.1 Initial conditions

Initially black oil feed is defined as 100% oil and initially reservoir is considered to be completely saturated with oil. The pressure in the reservoir is 130 bar and the temperature is 100°C.

### 4.2.5.2 Pressure boundary (well)

Mesh is divided into 10 sections along the x-axis. The well also lies parallel to the x-axis. Therefore the well is also divided into 10 zones. For each zone, the position of the well, its radius, and the main direction of flow have to be defined. As shown in Figure 4-1 the well is located at the center of the y-axis. Hence the y-coordinate of the will is 15. When considering the vertical axis, the well lies 6m below the top boundary. Therefore the z-coordinate of the well is 3 for all zones. The direction of the flow of the well is in x-direction and the diameter of the well is taken as 0.1 m. Pressure and the temperature of the well are respectively 130 bar and 100°C.

### 4.2.5.3 Pressure boundary (reservoir)

Reservoirs which are driven by water have an aquifer at the bottom of the oil reservoir. This boundary condition is defined in Rocx as, having a water feed at all the elements in the plane  $z = 20\text{m}$  (10<sup>th</sup> element of z). Pressure and the temperature of this boundary are 130 bar and 100°C respectively. The direction of this drive is in z-direction.

## 4.2.6 Simulation

Simulation of the reservoir model was carried out using an iterative linear solver named 'Linsolver'. Minimum time step was set to 100s while the maximum time step was set to 3600s. Initial time step was set to as 0.01s.

## 4.3 Development of the well and wellbore model

The model of the well was developed using the OLGA GUI environment. Main steps involved in developing the model are described below.

### 4.3.1 Case definition

Under case definition basic parameters and models required for the computation have to be defined. The simulation is conducted as a dynamic three phase system. Blackoil model is used as the compositional model. A first order discretization scheme is followed in solving the mass equations. For the simulations maximum and minimum time steps are 3600s and 100s respectively. The cases were simulated for 300 days.

### 4.3.2 Compositional

Under the compositional section blackoil components and black oil feeds have to be defined. These components have to be identical to the blackoil components and blackoil feeds that have defined in the reservoir model in Rocx. Under blackoil options, same Lasater model, GOR value etc, have to be defined according to the reservoir model.

### 4.3.3 Flow component

#### 4.3.3.1 Wellbore – pipeline model

To represent the wellbore a pipe with a length of 992m and diameter of 0.1m was taken and its roughness was set as  $2.8e-05$  m. The reservoir model has discretize the well into 10 zones, and each zone is divided into two sections. As a result the well is divided in to 20 hypothetical sections. A pipe with the same dimensions was taken to represent the base pipe and its roughness was defined as 0.045m. Similar to the wellbore, it is also divided into 20 sections. By using Figure 4-8 , which shows a single zone of the well, the concept of this model can be described.

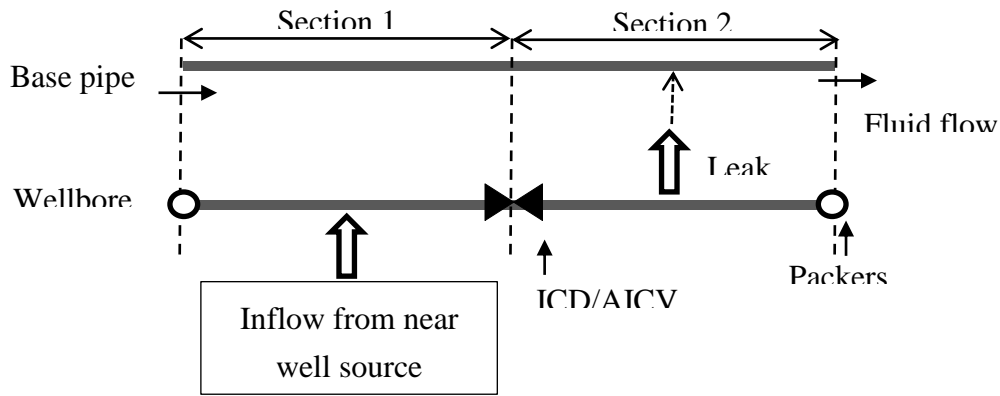


Figure 4-8: Simplified model of a single section of the well

Inflow that is coming from the reservoir enters the pipeline which represents the wellbore from section 1. This fluid flow has to go through an ICD or AICV in order to flow into the base pipe. After that it flows into the second section of the wellbore. Fluid enters the base pipe via a leak which is connected into the second section of the base pipe. In the wellbore, the pipe is separated by packers which do not allow the inflow from a one zone of the annulus to flow into a different zone in the annulus. But in the pipeline fluid flows from one zone to another. In Table 4-6 it is described how the model in Figure 4-8 is developed within OLGA GUI environment by using inbuilt OLGA modules.

Table 4-6: Reservoir/well model in OLGA

Component	OLGA module	Description
Inflow source	Nearwell source	Reservoir model (Rocx file) is coupled with this.
Leak	Leak	Diameter – 3.5 cm , $CD^1 - 1$ NO mass transfer between the phases. Connects to the pipeline
ICD/AICV	Valve/PID Controlled valve	Valve size is used to decide the required pressure drop through the ICD (typically 20mm). $CD - 0.84$ For AICV, valve opening is controlled through a PID controller.
Packers	Valve (closed)	Opening – 0 (fully closed), Diameter – 0.1 m

The boundary conditions of the wellbore and the base pipe have to be defined according to Table 4-7

<sup>1</sup> CD – coefficient of discharg



Table 4-7: Boundary conditions of the flow paths

Flow path	Boundary	Boundary type
Wellbore	Inlet	Closed
	Outlet	Closed
Base pipe	Inlet	Closed
	Outlet	Pressure boundary Pressure – 120 bar, Temperature – 100 <sup>0</sup> C

#### 4.3.3.2 AICV modeling

As AICV is an autonomous device which opens or closes itself according to the type of fluid which passes through it. To model an AICV in the simulation a valve controlled by a PID controller is used. By using transmitter module in OLGA, watercut percentage at the inlet section of the AICV which is the controlling parameter is measured and measured data is sent to the PID controller. Similar PID controlling system is used to choke the total flow rate of the system when ICDs are being simulated. Parameters of the PID controller are defined as in Table 4-8 to get a decent controlling performance over the controlled variable. These parameters are obtained by using trial and error method.

Table 4-8: PID controller parameters

Parameter	Value (AICV)	Value (for flow choking in ICD)
Amplification	-0.01	-0.0001
Bias (Initial signal)	1	1
Integral constant (s)	50	500
Maximum signal (maximum opening)	1	1
Minimum signal (minimum closing)	0.01	0.01

## 4.4 Simulated cases

Among the three types of reservoirs mentioned in 4.2.3, fractured reservoir was more focused in conducting simulations. Due to its high permeable zone, an early breakthrough is expected. Such an environment is favoured in studying the capabilities of different inflow control techniques in controlling water inflow.

Three main cases were simulated, focusing on three different types of inflow control technologies which are listed in Table 4-9. A reference case having ICDs with 20mm opening, and without choking the total flow was also simulated. Results obtained by the three main cases were compared with respect to the reference case. The intention of not choking the total flow is to understand the reservoir's potential in producing oil and water when required controlling actions are not implemented.

*Table 4-9: Types of inflow control technologies*

<b>Case</b>	<b>Description</b>
Case 1 (ICD <sub>ch</sub> )	Well having ICDs (20mm opening) combined with choking of the total flow from the reservoir.
Case 2 (ICD <sub>ch,res</sub> )	Installing an ICD having a relatively higher flow restriction at the high permeable zone while installing normal ICDs in the rest of the zones. Total product rate is also choked when the total flow rate exceeds the desired value.
Case 3 (AICV <sub>1%</sub> )	Well with AICVs having a relative opening of 1% when the AICV is in closed position.

Based on the results obtained by these simulations, several new cases were designed and simulated by combining the positive features of Case 2 and Case 3. Once the effective methods of controlling water inflow were identified, those inflow control technologies were applied to heterogeneous and homogeneous reservoirs to see whether the same performances can be achieved.

To analyse and compare the results of the different cases, following data from the simulations were taken into consideration.

- Accumulated total liquid, oil and water flow (m<sup>3</sup>) with time
- Volumetric flow rate of total liquid, oil and water with time (m<sup>3</sup>/day)
- Frictional pressure drop along the pipeline with time
- Pressure distribution along the pipeline with time
- Relative valve opening of the AICVs and choking valves
- Measurement signal of the PID controllers

## 5 Development of the numerical model

### 5.1 Background

The unique functionality of AICV is its capability to stop the flow when a low viscous fluid tries to go through it. AICV is designed with a reversible function to be reopened when the low viscous fluids are replaced by the high viscous fluids due to gravity. Time taken for an AICV to be reopened is an important parameter which can affect economic operation of a well. The objective of developing a simple numerical model is to estimate the time required for an AICV to be reopened when gas breakthrough occurs.

### 5.2 Assumptions

- Vertical and horizontal permeabilities of the reservoir are constant.
- Reservoir pressure, well pressure, reservoir and fluid properties are constants and do not change with time.
- Density and viscosity of the gas are taken from the properties of methane at reservoir conditions.
- Both gas and oil behave as incompressible fluids as there is not enough driving force to compress the fluids.
- Initially the wellbore is completely filled with oil. When gas enters into the wellbore, total volume of the wellbore is completely occupied by the two fluids.
- AICV is represented by an opening at the bottom of wellbore tube. This opening has the same length as the wellbore and it lies parallel to the axis of the wellbore. This is illustrated in Figure 5-4.
- When the AICV is closed it restricts the oil flow down to 1% of its initial oil flow rate (when the AICV is opened).

### 5.3 Conservation of mass within the wellbore

The basic mass balance can be applied to the wellbore as follows,

$$\frac{dm_{\text{wellbore}}}{dt} = \dot{m}_{\text{in}} - \dot{m}_{\text{out}}$$

As the volume is occupied by the two phases, mass balance can be applied to the two fluids separately.

For oil,

$$\frac{dm_o}{dt} = \dot{m}_{o\_in} - \dot{m}_{o\_out} \quad (5.1)$$

For gas

$$\frac{dm_g}{dt} = \dot{m}_{g\_in} - \dot{m}_{g\_out} \quad (5.2)$$

Since the densities of gas and liquid are assumed to be constant, equation (5.1) and (5.2) can be rewritten as,

For oil,

$$\frac{dV_o}{dt} = \dot{V}_{o\_in} - \dot{V}_{o\_out} \quad (5.3)$$

For gas,

$$\frac{dV_g}{dt} = \dot{V}_{g\_in} - \dot{V}_{g\_out} \quad (5.4)$$

By combining the equations (5.3) and (5.4)

$$\frac{d(V_o + V_g)}{dt} = (\dot{V}_{o\_in} + \dot{V}_{g\_in}) - (\dot{V}_{o\_out} + \dot{V}_{g\_out}) \quad (5.5)$$

According to the assumption made, total volume of the wellbore is occupied by the two fluids at any given time. Therefore,

$$V_o + V_g = V_{wellbore}$$

Hence (5.5) can be rewritten as,

$$\frac{dV_{wellbore}}{dt} = \dot{V}_{in} - \dot{V}_{out}$$

And as the volume of the annulus does not change with the time,

$$\begin{aligned} \frac{dV_{wellbore}}{dt} &= 0 \\ \dot{V}_{in} &= \dot{V}_{out} \end{aligned} \quad (5.6)$$

At any given time, (5.7) is true for the wellbore

$$\dot{V}_{o\_in} + \dot{V}_{g\_in} = \dot{V}_{o\_out} + \dot{V}_{g\_out} \quad (5.7)$$

The next step in developing this flow model is to derive functions for the volumetric inflows and outflows of the two fluids.

## 5.4 Inflow to the wellbore

Driving force for both gas and oil inflow is the pressure difference between the reservoir and well. When the AICV is closed, this driving force no longer exists. Oil and gas inflow to the

wellbore will be restricted as there is no driving force for the flow to be continued. However due to hydrostatic pressure difference, a small oil and gas flow will be driven into the wellbore. Therefore two different inflow profiles have to be used in this model, depending whether the AICV is opened or closed.

## 5.4.1 When AICV is opened

### 5.4.1.1 Gas inflow

In Figure 5-1 a schematic diagram of gas coning is shown. When gas coning occurs, it happens at a limited area on the top part of the wellbore.

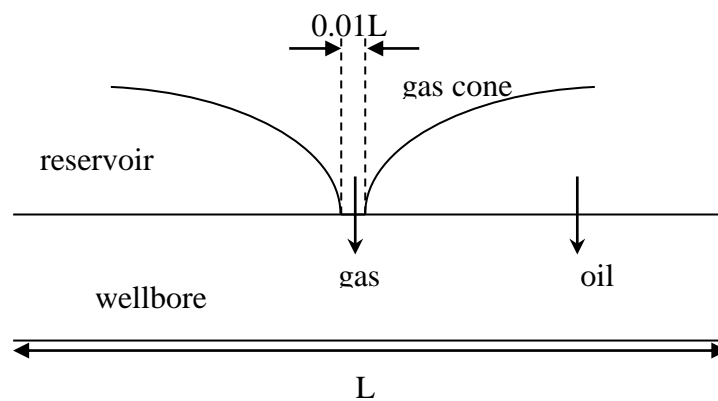


Figure 5-1: Gas coning

As it does not occupy the whole perimeter of the wellbore, it is assumed that the linear Darcy flow model can be applied to determine the gas inflow to the well. Hence the volumetric gas flow into the wellbore is given by

$$q_{g\_in} = \frac{k_v A}{\mu_g} \cdot \frac{(P_e - P_w)}{r_e - r_w} \quad (5.8)$$

Where,  $A$  is the area of the interface between the wellbore and gas cone which is shown in Figure 5-2. The thickness of the cylindrical section ( $l$ ) which is in contact with the gas cone is taken as 1% of the total length of the considered well (as seen as in Figure 5-1)

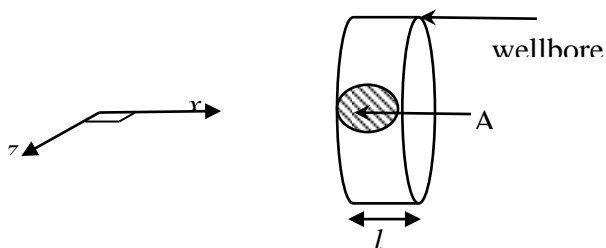


Figure 5-2: Wellbore- gas cone interface

Hence the wellbore-gas cone interface can be expressed as,

$$A = \pi \frac{(0.01L)^2}{4}$$

And therefore (5.8) can be written as,

$$q_{g\_in} = \frac{\pi k_v (0.01L)^2}{4\mu_g} \cdot \frac{(P_e - P_w)}{r_e - r_w} \quad (5.9)$$

#### 5.4.1.2 Oil inflow

Equations from (3.4) to (3.6) are used to calculate the flow rates of oil, that is coming into the wellbore from the reservoir.

$$q_{o\_in} = \frac{k_H h \Delta P}{141.2 B \mu \left( \ln \left\{ \frac{a + \sqrt{a^2 - (L/2)^2}}{L/2} \right\} + \left( \frac{l_{ani} h}{L} \right) \ln \left\{ \frac{l_{ani} h}{[r_w (l_{ani} + 1)]} \right\} \right)} \quad (3.3)$$

$$l_{ani} = \sqrt{\frac{k_H}{k_v}} \quad (3.4)$$

$$a = \frac{L}{2} \left\{ 0.5 + \left[ 0.25 + \left( \frac{r_{eH}}{L/2} \right)^4 \right]^{0.5} \right\} \quad \text{for } \frac{L}{2} < 0.9 r_{eH} \quad (3.5)$$

### 5.4.2 When the AICV is closed

#### 5.4.2.1 Gas inflow

The new driving force is the hydrostatic pressure gradient and it can be simply expressed as,

$$\Delta P = (r_e - r_w) \rho_g g$$

Based on the gas inflow rate on (5.9), the new gas inflow rate can be expressed as,

$$q_{gi,c} = q_{g\_in} \cdot \frac{(r_e - r_w) \rho_g g}{(P_e - P_w)} \quad (5.10)$$

#### 5.4.2.2 Oil inflow

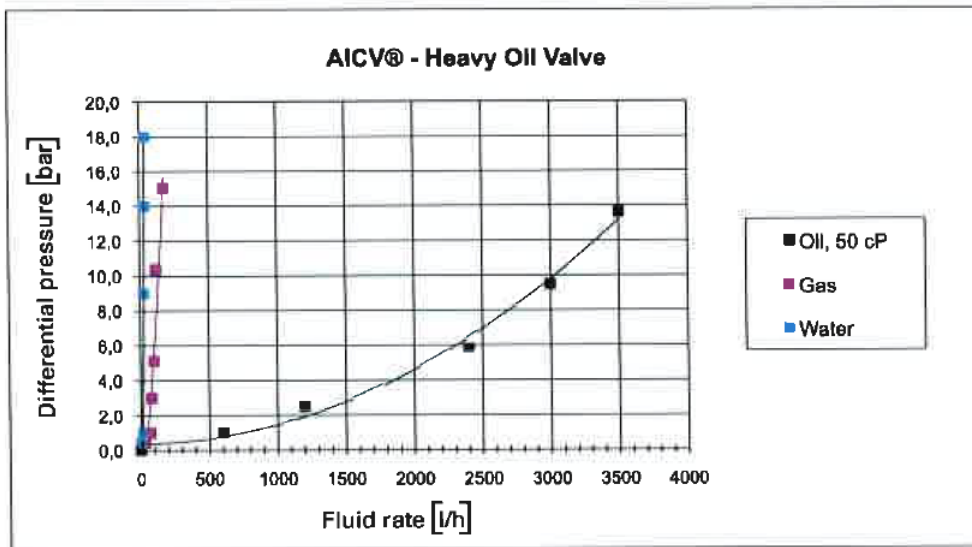
Based on the same method applied for the gas inflow, a new oil inflow profile can be derived. It is assumed that only the upper part of the wellbore contributes for this flow and no oil will flow into the reservoir from the bottom of the wellbore. The new oil inflow rate can be expressed as,

$$q_{oi,c} = \frac{q_o}{2} \cdot \frac{(r_e - r_w) \rho_g g}{(P_e - P_w)} \quad (5.11)$$

## 5.5 Outflow from the wellbore

### 5.5.1.1 When the AICV is opened

In Figure 5-3 flow performance curve for AICV is given. Based on this the outflow from the reservoir can be modelled. The outflow profiles should always satisfy the condition in (5.7).



Flow performance curve for AICV® heavy oil valve.

Figure 5-3: Flow performance curve for AICV

If the total pressure difference between the reservoir and wellbore exists across the AICV, the maximum outflow will be achieved. If the oil inflow calculated from (3.4) is less than the maximum possible outflow from the AICV, the actual outflow of oil can be calculated as,

$$q_{o\_out} = q_{o\_in} \quad (5.12)$$

The wellbore is completely filled with oil initially. Therefore until the wellbore is completely filled with gas, gas will not reach the AICV and until that gas outflow will be zero.

$$q_{g\_out} = 0 \quad (5.13)$$

### 5.5.1.2 When the AICV is closed

Eventhough the AICV is closed, according to section 2.3.2 ,a pilot will flow through it. It is assumed that it will allow 1% of initial oil flow to go through the valve. Therefore when the valve is closed, oil out flow can be expressed as,

$$q_{o\_out,c} = \frac{q_{o\_in}}{100} \quad (5.14)$$

Then from (5.7) gas outflow can be expressed,

$$q_{g\_out,c} = q_{oi,c} - q_{o\_out,c} + q_{gi,c} \quad (5.15)$$

It is assumed that no gas flow will go back to the reservoir and all the gas will go into the base pipe.

## 5.6 Time taken to reopen AICV

### 5.6.1 Equivalent wellbore tube

In

Figure 5-4 (a) schematic diagram of the wellbore and the base pipe is presented. An equivalent cylindrical tube is defined to represent the wellbore annulus which is shown in Figure 5-4 (b). Both the actual wellbore annulus and the equivalent wellbore tube have equal lengths and volumes.

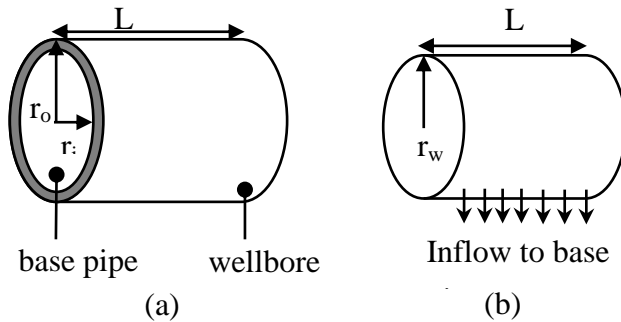


Figure 5-4: Equivalent wellbore tube

Radius of the equivalent wellbore tube can be defined as follows.

$$V_{wellbore} = \pi(r_{ow}^2 - r_{iw}^2)h = \pi r_{we}^2 h$$

$$r_{we} = \sqrt{r_{ow}^2 - r_{iw}^2} \quad (5.16)$$

### 5.6.2 Time for the wellbore to be filled with gas

Simulation is initiated when the first gas bubble enters the wellbore ( $t=0$ ). Time taken for wellbore to be completely filled with gas can be calculated by,



$$t_{close} = \frac{V_{wellbore}}{q_{g\_in}} = \frac{\pi r_{we}^2 h}{q_{g\_in}} \quad (5.17)$$

Where  $q_{g\_in}$  is calculated from (3.4). Equation (5.17) is valid as the volumetric inflow and outflow of oil is equal when the valve is opened.

### 5.6.3 Time taken for the gas to exist from the wellbore

AICV is designed to be reopened when high viscous fluid enters into it. In this model, it is expected to be reopened when the wellbore is filled with oil. When the reservoir is filled with oil, it can enter into the AICV to cause the required pressure drop to reopen it. Therefore time taken to reopen the AICV can be expressed as,

$$t_{reopen} = \frac{f_{V,reopen} V_{wellbore}}{q_{g\_out,c} - q_{gi,c}} \quad (5.18)$$

## 5.7 Calculation

A simple calculation is conducted based on the developed model for a general gas breakthrough situation. The calculation procedure is presented in Appendix 6: Numerical model calculation. Parameters used for the calculations are listed in Table 5-1.

*Table 5-1: Parameters for the numerical model*

Property	SI units	Imperial units	Property	SI units	Imperial units
$r_e$	3 m	9.8425 ft	$P_w$	110 bar	1595.415 psi
$r_{ow} = r_w$	0.1 m	0.328 ft	$k_H$	9.869e-13 m <sup>2</sup>	1000 mDa
$r_{iw}$	0.09 m	0.295 ft	$k_V$	9.869e-14 m <sup>2</sup>	100 mDa
$r_{eH}$	40 m	131.234 ft	$\mu_o$	0.15 Pa.s	150 cp
$L$	12.4 m	40.682 ft	$\mu_g$	15.744e-6 Pa.s	0.015744cp
$h$	12 m	39.37 ft	$B_0$	1.1[-]	1.1[-]
$P_e$	120 bar	1740.453 psi			

The results obtained by these calculations are summarized in Table 5-2.

*Table 5-2: Results obtained by numerical model calculations*

$q_{g\_in}$	0.094 m <sup>3</sup> /hr
I <sub>ani</sub>	3.16
a	132.02 ft
$q_{o\_in}$	0.298 m <sup>3</sup> /hr
$q_{oi,c}$	3.9e-03 m <sup>3</sup> /hr
$q_{gi,c}$	1.755e-04 m <sup>3</sup> /hr
$q_{o\_out,c}$	2.98e-03 m <sup>3</sup> /hr
$q_{g\_out,c}$	1.095e-03 m <sup>3</sup> /hr
$t_{close}$	0.788 hr
$t_{reopen}$	3.3 days

## 6 Simulation results

To study the functionality of AICVs under different conditions, the results obtained from the simulations are illustrated and analysed. It is essential to have a thorough understanding of the oil and water production capability of the reservoir in conducting such an evaluation. By analysing the case that is used as the reference case in OLGA-Rocx simulations, the reservoir's potential in producing oil and water can be evaluated.

### 6.1 Analysis of the reference case

Oil and water production potential of the fractured reservoir (Figure 4-7 (a)) can be evaluated by studying the accumulated oil and water volumes of the reference case. In Figure 6-1 accumulated volumes of oil, water and total liquid are presented with respect to time.

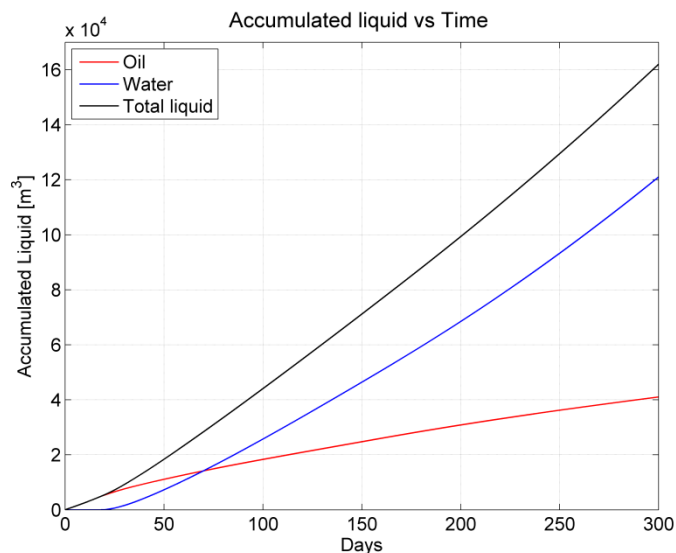


Figure 6-1: Accumulated liquid flow of the reference case

According to Figure 6-1 an early water breakthrough occurs on the 18<sup>th</sup> day of operation. Once water has started to be produced, the reservoir has a tendency to produce more water than oil. As a result, accumulated volume of water is twice as the volume of the accumulated oil, after 300 days. This implies that the reservoir has produced oil with high water cut which is not suitable for an economical production.

Liquid flowrates and the water cut diagrams in Figure 6-2 show that, as soon as the water breakthrough occurs after 18 days, oil production rate has been significantly reduced. However due to the higher water production rate, total liquid flow rate is continuously increasing. On the 30<sup>th</sup> day water production rate exceeded the oil production rate, causing the reservoir to produce more water than oil. After 160 days a gradual increase in the water cut diagram is observed. Similarly a gradual increment in water flowrate is also observed after

160 days. This implies that a second water breakthrough has occurred in the considered case.

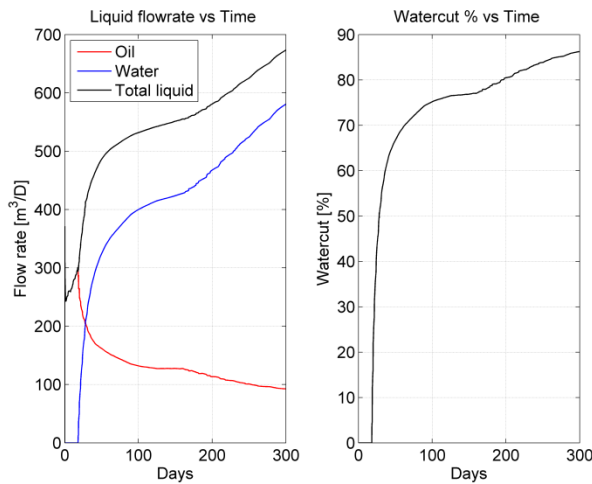


Figure 6-2: Liquid flow rates and water cut % of the reference case

As the simulated reservoir has a high permeable zone and 9 less permeable zones, two water breakthroughs are expected. The first water breakthrough should occur at the high permeable zone while the second breakthrough should occur through the rest of the zones. This phenomena can be seen by the oil saturation profile of the reservoir. Oil saturation profiles of the 10 zones, on the 18<sup>th</sup> day of operation are shown in Figure 6-3. According to that the water breakthrough has occurred only at the 4<sup>th</sup> zone where the permeability is high. In the other zones water has barely entered into the reservoir.

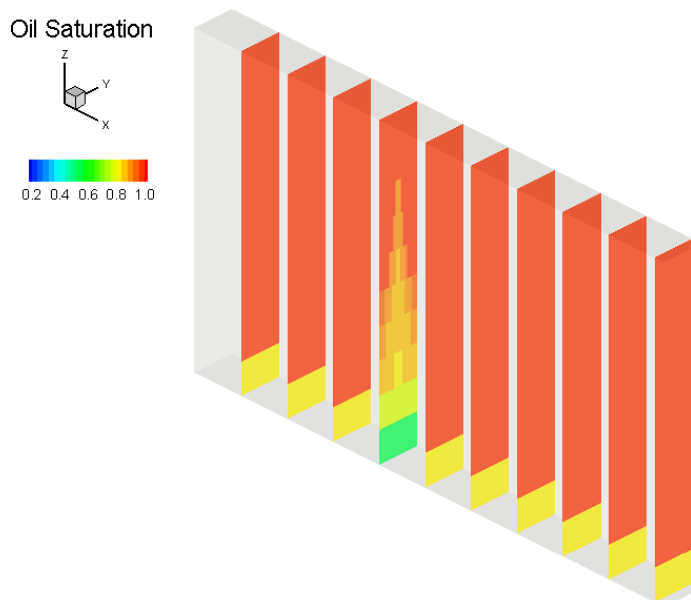


Figure 6-3: Oil saturation profile after 18 days (base case)

Oil saturation profiles of the yz-planes in zone 10(heel),6 and 1(toe) are shown in Figure 6-4. These are obtained on the 160<sup>th</sup> day of the operation. In zone 10 a conical shaped saturation

profile is obtained which known as the water cone. Practically when a water breakthrough occurs, a conical shaped water saturation profile is obtained within the reservoir. Hence it can be argued that, physically acceptable results are obtained by the simulations. When compared to the heel section, water cones in the zone 6 and in toe section are still developing. This is due to the heel-toe effect in horizontal wells.

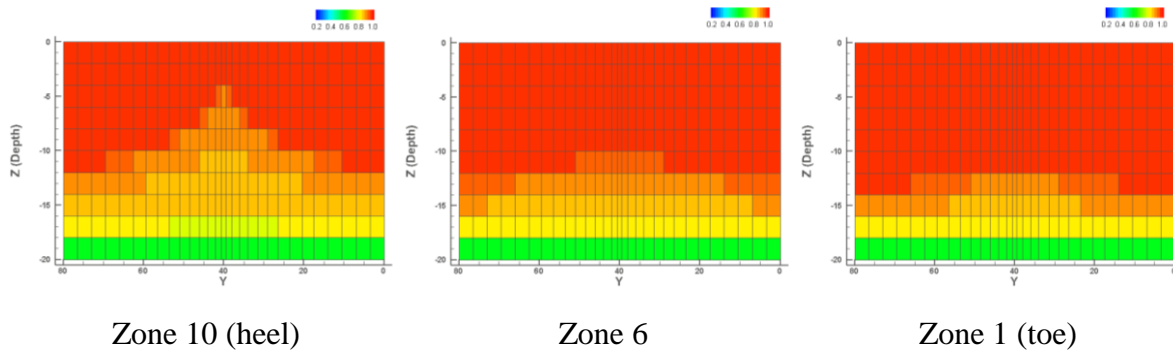


Figure 6-4: Oil saturation profile in the reference case after 160 days

In this reservoir an early water breakthrough takes place via a single zone where the permeability is the highest. Once the water breakthrough occurs, water flow rate will exceed the oil flow rate due to the high permeability in the water breakthrough zone, regardless of the oil production from the rest of the zones. To extract an oil product with a low water cut level, it is essential to install better inflow control instruments. Based on this reference case it can be seen how different forms of AICVs and ICDs affect the water inflow from the reservoir. In this study normal ICD and is having an diameter of 20mm and a normal AICV is having an opening diameter of 20mm and 1% minimum opening at the closed position.

## 6.2 Comparing the basic performances of AICVs and ICDs

### 6.2.1 Accumulated water and oil

Accumulated oil and water are two of the most important parameters that have to be taken into consideration when comparing the performances of different inflow control technologies. In Figure 6-5 accumulated volumes of oil and water are plotted for the cases mentioned in Table 4-9.

According to the Figure 6-5 it is observed that all the considered inflow control technologies have the capability to reduce the water inflow down to different values. Among the considered inflow control technologies, AICVs have the highest potential in reducing the water inflow. On the other hand, normal ICDs with choked flow have reduced the accumulated oil volume significantly, while the other two methods have been deviated from the reference case slightly.

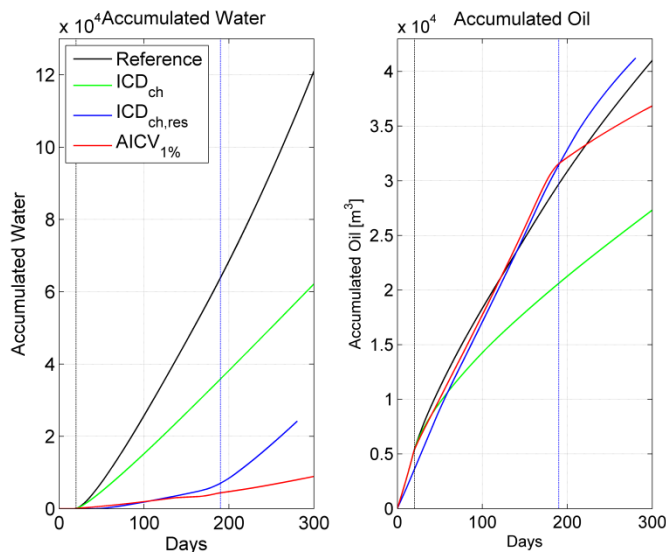


Figure 6-5: Accumulated oil and water for comparison

The deviations of the accumulated oil and water volumes, of the different inflow control technologies, can be expressed with respect to the reference case. The relative deviations and the average water cut, of the total flow are summarized in the Table 6-1. These results were obtained on the 280.5<sup>th</sup> day of the operation.

Table 6-1: Accumulated oil comparison

Case	Change of oil accumulation [%]	Change of water accumulation [%]	Average water cut [%]
ICD <sub>ch</sub>	-33.23	-47.7	68.71
ICD <sub>ch,res</sub>	5.23	-77.94	37.01
AICV <sub>1%</sub>	-8.05	-92.71	18.18

The restrictions imposed on the fluid inflow to control the water production, have affected a reduction in oil production as well. Based on the amount of accumulated water, AICVs display a remarkably higher potential in restricting the water inflow.

By considering the results obtained from Case 1, it can be seen that by choking the total flow will not only reduce water production but will also limit the oil production. When it comes to quality of the final product, the reference case has an average water cut of 73.71%. This simulation shows that having relatively low restrictive uniform ICDs with flow choking does is not a suitable solution for the water inflow problem in fractured reservoirs.

It is interesting to see that by replacing the normal ICD in the high permeable zone with a more restrictive ICD, the results have been dramatically changed. It has enhanced the accumulated oil volume while the other two inflow control technologies have reduced the amount of oil production, compared to the reference case. According to Figure 6-5, until the

second breakthrough occurs on the 160th day, flow pattern of the AICV case and the nonuniform ICD case ( $ICD_{ch,res}$ ) follow a similar similar path.

As both AICV and nonuniform ICD have a satisfying potential to control the water inflow causing only a slight disturbance over the oil production rate, thier positive and negative features have to be further examined.

## 6.2.2 Oil and water flow rates

Changes of the oil and water flow rates throughtout the production time , specially when the water breakthrough takes place, will indicate the positive and negative features of the AICV and nonuniform ICD methods. Based on the Figure 6-6 which is showing the oil and water flow rates, features of the AICV and nonuniform ICD systems are explained.

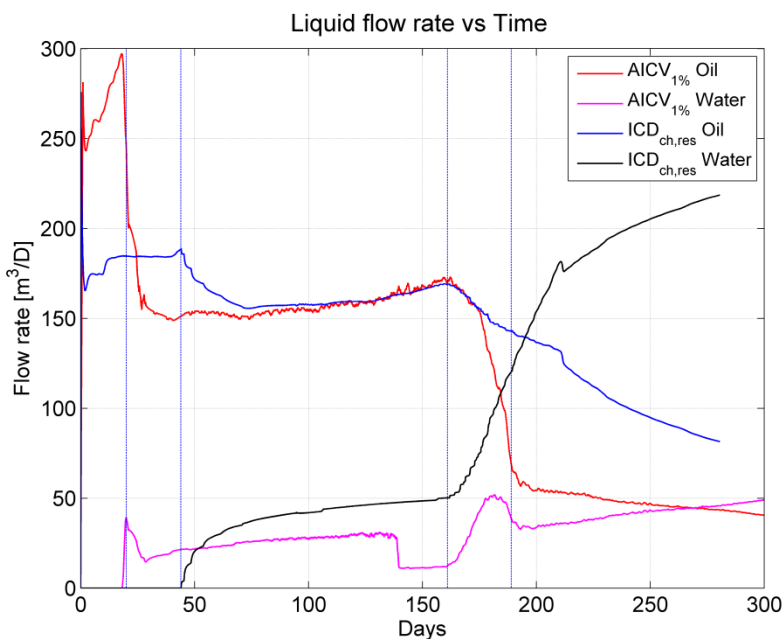


Figure 6-6: Oil and water flow rate of AICV and  $ICD_{ch,res}$  methods

It can be seen that by installing a more restrictive ICD having a higher pressure drop, in the high permeable zone, the early water breakthrough has been delayed down to 44 days. Due to the higher pressure though the new ICD ,oil production rate has also been reduced. Since the first breakthrough has been delayed, it is interesting to observe the amount of oil that has been accumulated when the breakthrough takes place. In the Table 6-2, the amount of accumulated oil at the time of the breakthroughs are summarised.

Table 6-2: Oil production at the breakthroughs

Case	First breakthrough	Amount of oil Produced at the first breakthrough	Second breakthrough	Amount of oil Produced at the first breakthrough	Amount of oil Produced at the first breakthrough
ICD <sub>ch</sub>	18 days	4928.76	160 days	18627.7	28844.18
ICD <sub>ch,res</sub>	44 days	8056.73	160 days	26804.67	4624.76
AICV <sub>1%</sub>	18 days	4928.76	160 days	27451.04	3305.26

These data suggest that the nonuniform ICD method has the capability to produce more oil at the time of breakthrough. Nonuniform ICD method has been able to produce 63.46% more oil compared to uniform ICD and AICV methods, at the time of the breakthrough. This can be considered as the most important positive feature of the nonuniform ICD method. Its negative features are the low oil production rates and the inability to control the water inflow when the breakthrough happens. From a practical point of view, it is difficult to locate the exact position of the high permeable zones and hence it is challenging to install more restrictive ICDs within particular zones.

Even though nonuniform ICD method has been able to delay the first breakthrough, by the time of the second breakthrough happens, it has produced more water and less oil compared to AICV system. It shows that the AICV's have better inflow controlling capability which is its most important positive feature. In Figure 6-6 it can be observed that when the second breakthrough happens on the 160th day, oil production rate rapidly reduce and water flow rate rapidly increases. When observing the relative opening area of the AICVs with respect to time, it takes 20 days for them to reach the closed position (minimum opening). If an AICV takes relatively a long period of time to reach its closed position, water production rate will also be increased. At the same time, if an AICV has a relatively a very small opening at the closed position, oil production rate will also be reduced significantly along with the water inflow rate. As a result the amount of oil being produced after the valves are closed down, is less than the nonuniform ICD method. This is a factor which has to be considered based on the economics of the production. With a smaller opening of the the AICV, both oil and water flow rates will be reduced and if the opening area of the valve is set to a higher value at the closed position, it will increase the water and oil production rates.



# 6.3 Effects of design parameters of AICV

## 6.3.1 Pressure drop and minimum opening area

In an AICV, pressure drop across the valve and the allowable flow at the closed position are design parameters, which can be adjusted depending on the application. Based on the results obtained in chapter 6.2, it was observed that, if an ICD with a higher pressure drop, can be installed in the high permeable zone, first breakthrough can be delayed. It will also produce twice the amount of oil at the time of break through with respect to the reference case. It will also make sure that a less amount of water will be produced from the high permeable zone.

It was also observed that, as the AICV valves are closed down, oil production rate also declines significantly. However by installing an AICV with a lower opening, at the high permeable zone, will reduce the water inflow to the wellbore. Therefore two cases were simulated to see the effect of having a higher pressure drop over the AICV and the effect of having a better closing valve at the high permeable zone.

The accumulated oil and water profiles of these two cases are presented in Figure 6-7 with respect to the accumulated oil and water profiles of uniform AICVs with 1% minimum opening.

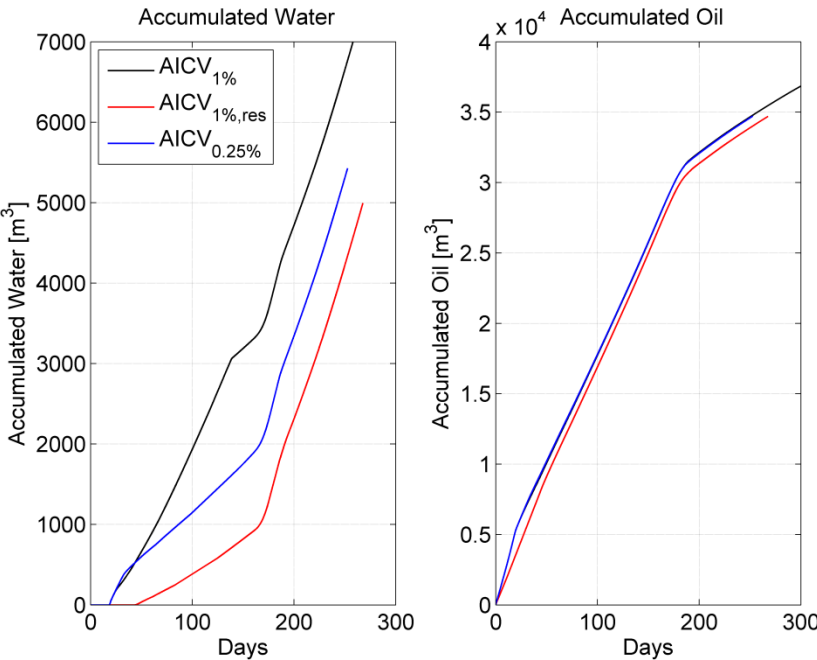


Figure 6-7: Accumulated water and oil wrt AICV parameters

When considering the amount of accumulated water, it can be concluded that having a higher pressure drop is more effective than having a fine closing. This phenomenon is highly dependable on the reservoir and fluid properties. In this particular well, by reducing the minimum opening down to 0.25% ,has no effect on the amount of oil accumulated. Having a higher pressure drop has also reduced the oil accumulation slightly.

If it is required to produce more oil at a higher production, minimum opening of the AICVs in the low permeable zones, have to be increased. A new case was simulated by having an AICV with both higher pressure drop and a lower opening at the high permeable zone and having AICVs with 2% opening in rest of the zones. The obtained results are plotted with respect to the results in Figure 6-7 and it is presented in Figure 6-8

As expected the new combination has yielded a higher oil production, but it has also increased the water production as well. The acceptable water cut and the minimum opening area of the AICVs have to be decided based on the economics of the production process.

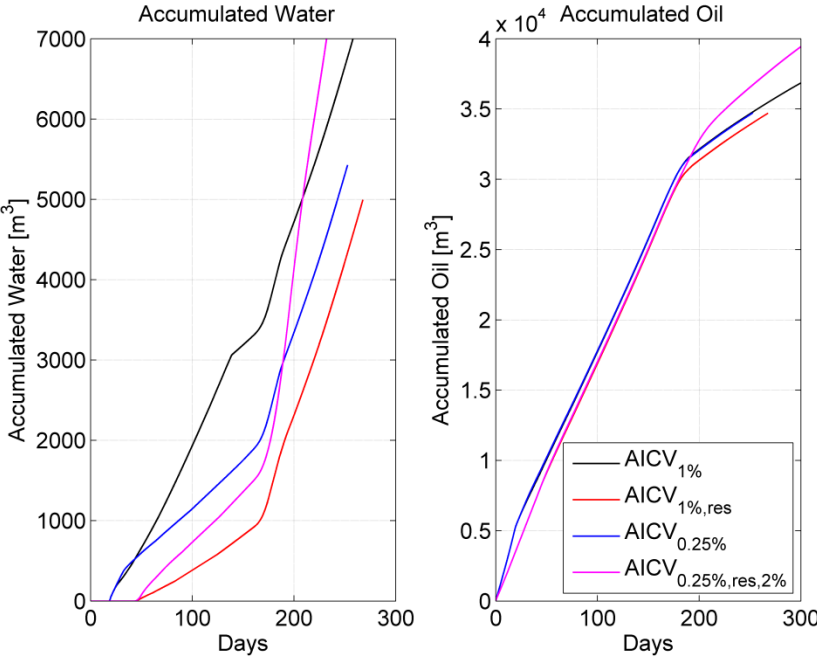
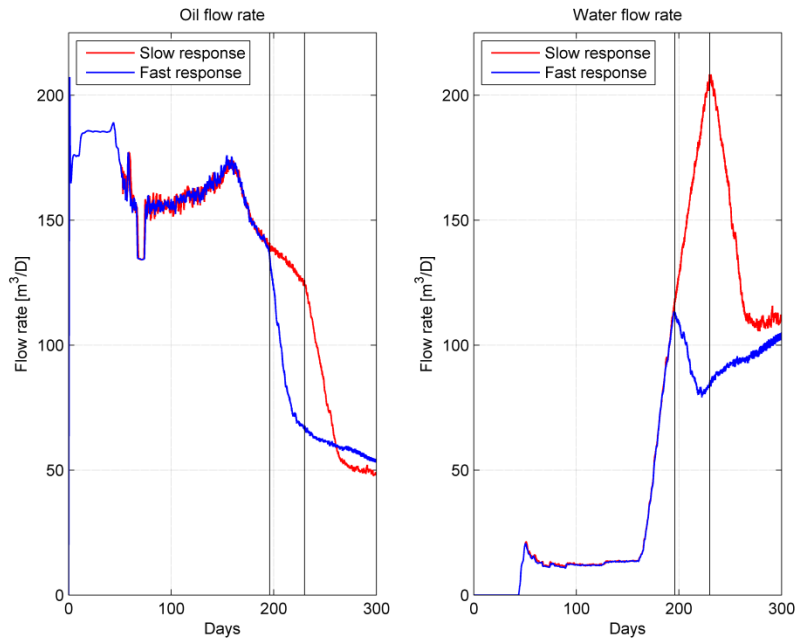


Figure 6-8: Accumulated oil and water with 2% opening AICV

### 6.3.2 Response time

Once the water starts to flood into the AICV, it takes a certain period of time for the valve to respond to the change of the fluid properties. As a result the valve will not close as soon as the water breakthrough occurs. In Figure 6-9 oil and water flow rates of two identical cases having AICVs with different response times are presented. As it can be seen, if the valve closes slowly, water production rate rapidly increases and as a result water accumulation will be increased. However after the AICVs reach their closed positions, both water and oil flow rates will reach the same value regardless of the response time.



*Figure 6-9: Oil and water flow rates under different response-times*

From a practical point of view the difference between the two response times might not be significant. But from a simulation point of view, PID controller which is used to represent the AICV has to be tuned properly. Otherwise closing will not be similar to the actual closing function of the AICV. As a result significant errors could occur in the accumulated flows.

## 6.4 Functionality of the AICVs and ICDs in homogeneous reservoirs

As AICVs have displayed better control in water inflow in fractured reservoirs, it is important to see whether the same superior performances can be observed in homogeneous reservoirs.

For the simulations, a reservoir with a vertical permeability of 100mDa was considered as shown in Figure 4-7. Accumulated oil and water quantities are plotted in Figure 6-10 and as expected, AICVs have reduced the amount of water that is being produced. According to the results obtained, AICVs have been able to reduce the water accumulation by almost 47%. As a side effect of the inflow control, oil production has also being reduced by 7%.

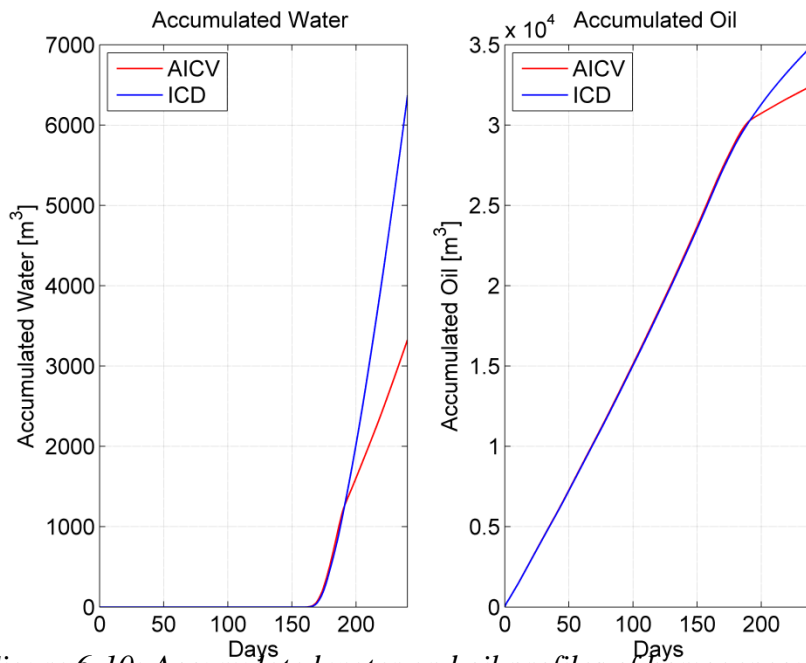


Figure 6-10: Accumulated water and oil profiles of homogeneous reservoir

As seen in Figure 6-10, until the AICVs are closed down, both ICDs and AICVs follow the same flow pattern. Once the AICVs are closed down both oil and water inflows are choked down. In a homogeneous reservoir, water breakthrough occurs throughout the reservoir at once. Then all the inflows will be choked by the AICVs. Therefore the oil accumulation will be less than the normal ICDs. The changes of liquid flow rates are shown in Figure 6-11.

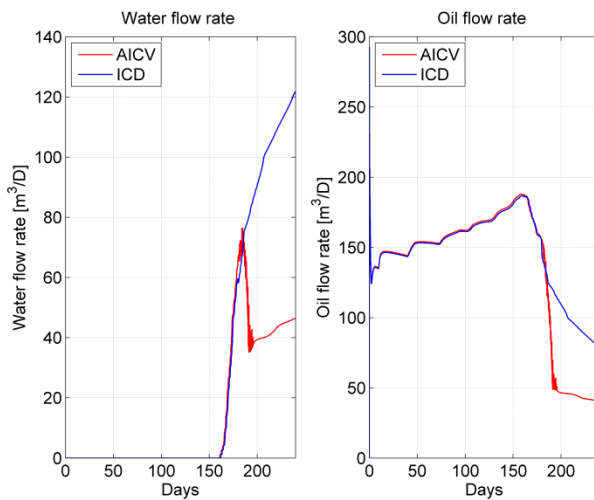


Figure 6-11: Water and oil flow rates of homogeneous reservoirs

ICDs have only been able to delay the water inflow and once the water starts flooding into the well it has no control over it. As a result water inflow rate is continuously increases while the oil production rate is gradually decreasing. Due to AICV's capability to restrict the inflow when the water starts flooding into the well, water flow rate is suddenly dropped down to a lower value, when the AICV is closed down. Due to the low viscosity of water, its production rate is gradually increasing. As a result when the valve is in the closed position where it cannot restrict the inflow further, water production rate will still be increasing. However

AICVs have been able to restrict the water inflow rate at a significantly lower value compared to the ICDs. As the AICVs are closed down, oil production is also rapidly reduced down and continuously decreases due to the production of water. After the valves are closed down oil production rate is relatively lower than the oil production rate with ICDs.

## 6.5 Functionality of the AICVs and ICDs in heterogeneous reservoirs

As shown in FIG, an intermediate reservoir between a fractured and a homogeneous reservoir was also taken for the simulations. The accumulated oil and water volumes are presented in Figure 6-12.

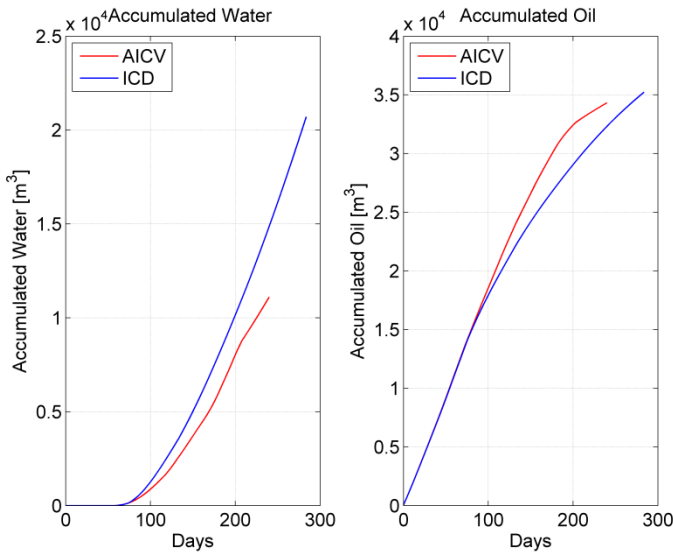


Figure 6-12: Accumulated water and oil profiles of heterogeneous reservoir

Compared to the accumulated liquid profiles in homogeneous reservoir AICVs in heterogeneous reservoirs have the potential to produce more oil with respect to ICDs. The liquid flow rate profiles of the considered heterogeneous reservoir are presented in FIG

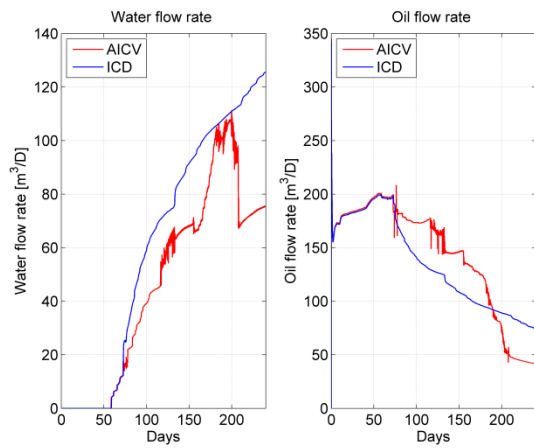


Figure 6-13: Water and oil flow rates of heterogeneous reservoir

As there are three different permeable zones three water breakthroughs occur during the production. First one occurs on the 55<sup>th</sup> day and the last one is initiated on 160<sup>th</sup> day. AICVs will be completely closed by the 210<sup>th</sup> day. That is why a sudden increase and decrease in water production rate is observed on 160<sup>th</sup> day and on 210<sup>th</sup> day respectively. Until the third breakthrough, AICVs have maintained a higher oil production rate. In the ICD system oil production rate has decreased due to the choking of the total flow.

By considering the results obtained for the three types of the reservoirs, AICVs can be effectively used in both fractured and heterogeneous reservoirs. Even though they reduce the water production in homogeneous reservoirs, they reduce the amount of oil produced as well.

In tab a simple comparison of the performance of normal AICVs and normal ICDs are present for the three reservoir types in Table 6-3

Table 6-3: Results summary (AICV vs ICD)

	Fractured	Heterogeneous	Homogeneous
Percentage change of oil accumulation with AICV (compared to ICD)	-86.95	-25.33	-47.66
Percentage change of water accumulation with AICV (compared to ICD)	43.99	6.19	-7.14
Percentage change of average water cut with AICV (compared to ICD)	-76.92	-22.42	-39.58

According to this AICV's performance is much better than the ICDs except in the oil production in homogeneous reservoirs. Based on this results it can be concluded that AICVs are ideal for fractured reservoirs and also for heterogeneous reservoirs.

# 6.6 Numerical model analysis

Based on the numerical model developed in Chapter 5, a simple study can be conducted on the factors affecting the time taken to reopen AICVs.

According to the model, time taken to reopen the AICV is linearly proportional to the viscosity of the considered oil. The relationship between the reopen time and oil viscosity is plotted in Figure 6-14.

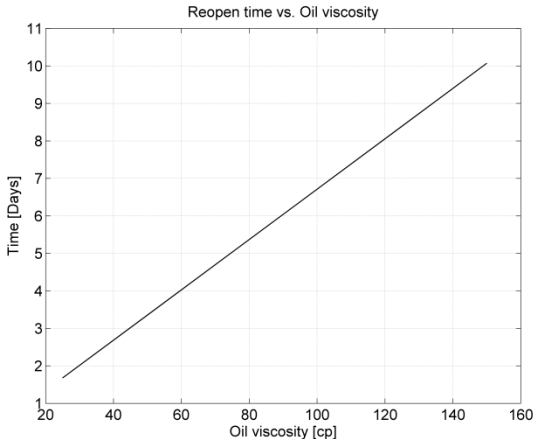


Figure 6-14: Reopening time vs. oil viscosity

As the viscosity of the oil increases, the rate of oil inflow to the wellbore is reduced. Therefore once the wellbore is filled with gas, it takes a longer time to replace the gas with oil having a higher viscosity.

In Figure 6-15 the relationship between the reopen time and the oil density is plotted.

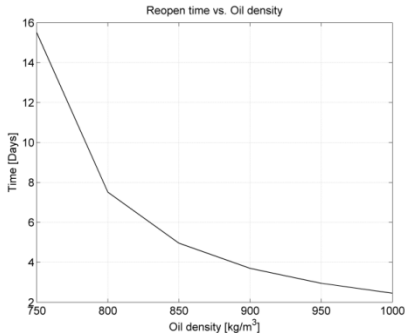
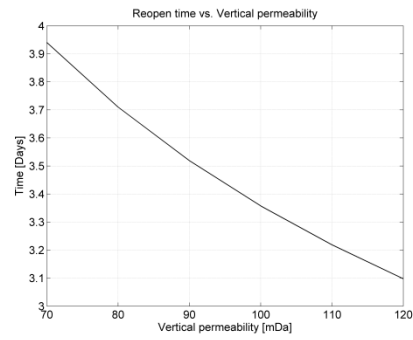
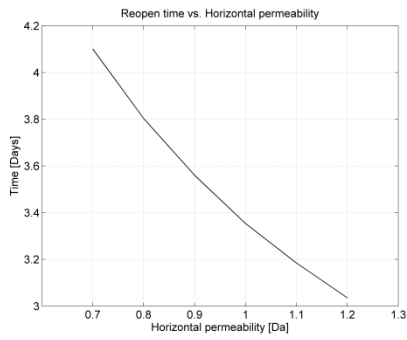


Figure 6-15: Reopening time vs. oil density

This simple model assumes that the flow into the wellbore, when the AICV is closed, is due to the hydrostatic pressure gradient. Hence heavy oil will inherit a higher flow rate when the AICV is closed. As a result the time taken to reopen the AICV will be reduced.

The effect of the vertical and horizontal permeabilities over the time taken to reopen the valve is plotted in Figure 6-16.



*Figure 6-16: Reopening time vs. Permeability*

Both permeabilities are inversely proportional to the time taken to reopen the valve. Fluid flow within a reservoir is enhanced when the permeability is increased and hence reducing the reopen time. When considering the sensitivity of the reopen time, it can be seen that it is relatively more sensitive to the changes in vertical permeability. As this is a horizontal well, gas inflow is proportional to the vertical permeability; hence the reopen time is more effected by the vertical permeability.

Size of the wellbore annulus also plays a major role in the time taken to reopen the valve. When the outer diameter of the well in increasing, time taken to reopen the AICV is also increased. On the other hand if the inner diameter of the annulus is increased, reopening time will be reduced. In well completion, different inner and outer diameter combinations can be taken in to consideration and it is important to see how that combination affects the functionality of the AICV.



## 7 Discussion

According to the results obtained by OLGA-Rocx simulations, AICVs best performance over controlling water inflow. Under all the conditions, which were taken into consideration during the simulations, AICVs have produced less water than all the other inflow control technologies.

Compared to the uniform ICD system, AICVs have been able to produce more oil in both fractured and heterogeneous reservoirs. In homogeneous reservoirs, as the AICVs choke the inflow of the all the zones simultaneously, oil production rate is reduced compared to the ICDs. This phenomenon can also be seen in the long run operation of heterogeneous and fractured reservoirs, when all the AICVs have been closed. By increasing the allowable flow through the AICV, when it is in closed position will enable to produce more oil considering the fact that it will produce more water as well.

It has been shown that if it is possible to install an AICV or and ICD having a relatively higher flow restriction, in the high permeable zone, early water breakthrough in fractured reservoirs can be delayed. It will also increase the amount of oil produce at the time of breakthrough takes place. A much lower water inflow rate can be achieved, compared to uniform AICV/ICD systems. The main drawback of this system is that is difficult to locate the exact location of the high permeable zones and it is also difficult to install a particular inflow control instrument in an exact location.

To conduct accurate simulations of the AICVs, it is important to tune the PID controlling system that is used to represent the AICV. False tuning will lead to slow responses or too many fluctuations, causing significant errors in the final results. Currently the tuning has to be conducted by trial and error method combined with PID condoling theory.

The numerical model which was developed to examine the valve reopen time is a very simple model which has to be compared with experimental data, before any modification is done. It shows that if the viscosity of the oil is high it will take a longer time to reopen the valve. It also suggests that high density oil will have a short reopen times. If the permeability of the reservoir is high, valve will be reopened much faster. However the effects of the compressibility of the gas, and the inflow rate to the wellbore when the AICV is closed have to be examined by conducting experimental work.

## 8 Conclusion

Based on the obtained results, it can be concluded that the AICVs can be successfully implemented to minimize the water inflow into the base pipe. Due to the choking of the inflow, AICVs will restrict the oil production down to a certain limit as well. By having a higher minimum opening area when the AICV is in closed position, restriction towards the oil production can be minimized. The acceptable limit of the water cut of the total water cut, has to be decided according to the economy of the production.

AICVs are more suitable to be used in heterogeneous and fractured reservoirs. In homogeneous reservoirs it will choke the oil inflow from all the zones and therefore the total oil production is rapidly reduced. If it is possible to have ICDs or AICVs having higher flow restriction properties, installed in the high permeable zone, much better inflow control action can be obtained. But practically it is difficult to install the correct type of AICV at the correct position.

Response time of the AICV plays a vital role in the effectiveness of the AICV. At the time of closing the AICVs, if the water flow rate is almost equal to the oil flow rate, reservoir will produce more water even after the inflows are choked. (due to the minimum allowable flow through AICV). For the simulations to be realistic, PID controller has to be tuned properly to represent the actual performance of the AICV.

All the results obtained by the simulations are required to be validated by conducting experimental work. And further study has to be conducted in homogeneous reservoirs, to see how the performance of the AICV can be enhanced.

According to the numerical model, once the AICV is closed down, it takes few days for it to be reopened. It is essential to study the flow behaviour of gas replacement by the oil as it has a significant impact on the model.

# Appendices

Appendix 1: Project task description

Appendix 2: Reservoir model in Rocx

Appendix 2: Relative permeability data

Appendix 4: Well/wellbore model in OLGA with AICV

Appendix 5: Well/wellbore model in OLGA with ICD

Appendix 6: Numerical model calculation

# Appendix 1: Project task description



**Telemark University College**

**Faculty of Technology**

## **FMH606 Master's Thesis**

**Title:** Near well simulation and modelling of oil production from heavy oil reservoirs

**TUC supervisor:** Prof. Britt Halvorsen

**External partner:** InflowControl AS, Vidar Mathiesen (co-supervisor)

**Task background:**

Heavy oil represents a massive world resource more than twice the size of global reserves of light or conventional oil. Different types of inflow control technologies are developed to increase oil recovery especially from heavy oil reservoirs. InflowControl AS is a technology company in the oil service that develops products and services related to increased oil recovery and production. The company has developed an autonomous inflow control valve (AICV) that will ensure an increased oil production and recovery. A better understanding of the multiphase reservoir condition is therefore required. In most reservoirs, oil, water and gas are present. Maximum oil production with minimum water and gas is the optimal case. Inflow control devices are capable of choking back or closing for unwanted gas and water in zones where breakthrough occurs, and oil can still be produced from the other zones of the well.

**Task description:**

In this project Rocx will be used for near well simulations. Rocx is a reservoir simulation program and is used in combination with OLGA to get the complete picture of fluid flow from reservoir to well and production pipe. OLGA-Rocx, can be used to calculate the production potential from different types of heavy oil reservoirs and to study the water coning in the reservoir.

The project will focus on:

1. Literature study of heavy oil production with water drive.
2. Perform near well simulations with OLGA-Rocx using different types of inflow control and water drive.
3. Comparing the different cases regarding oil production.
4. Development of numerical model


**Practical arrangements:**

Necessary software will be provided by TUC. Experimental work will be performed at InflowControl.

**Address:** Kjølnes ring 56, NO-3918 Porsgrunn, Norway. **Phone:** 35 57 50 00. **Fax:** 35 55 75 47.



**Signatures:**

  
Student (date and signature):

  
Supervisor (date and signature):

# Appendix 2: Reservoir model in Rocx

```
# Version: 1.2.2.0
# Input file created by Input File Editor.
# 5/30/2014 6:47:54 AM
# ModelDescription:Reservoir section 992X80X20 with pipeline at 6 mtr from top of reservoir section.
# Oil Viscosity: 150 cP
# Reservoir permeability: 0.1 Darcy
# Pressure in reservoir: 130 bar

*GEOMETRY RECTANGULAR

# Number of grid blocks in horizontal and vertical direction
# -----
# nx ny nz
# 10 29 10

dx const 99.2
dy j 3.5 3.5 3.5 3.5 3.5 3 3 3 2.5 2.5 2.5 2 2 1.5 1 1.5 2 2 2.5 2.5
2.5 3 3 3 3.5 3.5 3.5 3.5 3.5
dz const 2

# Direction vector for gravity
# -----
# gx gy gz
# 0 0 1

*FLUID_PARAMETERS

blackoil

# Black oil option data
# -----
gormodel Lasater
massfrac

rsgo_bp_tuning off

oilvisc_tuning on

gor 5
gasspecificgravity 0.64
oilspecificgravity 0.92
oilvisc 150
visctemp 100
viscpress 130

# Black oil component data
# -----
ncomp 3

label BO_Oil_0
type oil
oilspecificgravity 0.92

label BO_Gas_0
type gas
gasspecificgravity 0.64
# h2smolefraction Not used
# co2molefraction Not used
# n2molefraction Not used

label BO_Water_0
type water
waterspecificgravity 1

# Black oil feed data
# -----
nfeed 4
```

```

label Feed_3
oilcomponent BO_Oil_0
gascomponent BO_Gas_0
gor 5

watercomponent BO_Water_0
watercut 0.0001
label Feed_1
oilcomponent BO_Oil_0
gascomponent BO_Gas_0
glr 0.0001

watercomponent BO_Water_0
watercut 0.99
label Feed_2
oilcomponent BO_Oil_0
gascomponent BO_Gas_0
glr 0

watercomponent BO_Water_0
watercut 0
label Feed_0
oilcomponent BO_Oil_0
gascomponent BO_Gas_0
gor 0

watercomponent BO_Water_0
watercut 0

*RESERVOIR_PARAMETERS

# Porosity
# -----
por const 0.3

#      compr reference_pressure
rock_compr 0 0

# swc sor sgr
0 0 0

Pcow
0 1
1 0 /

Pcgo
0 0
1 1 /

*BOUNDARY_CONDITIONS

manual

# Injection flow rates
# -----
# nsource
0

# ix iy iz ntime time mw mo mg temp

# Production pressures
# -----
# npres_bou
11

# i j k idir type name ntime time pres_bou temp_bou Sw_bou So_bou Sg_bou Feeds
1-10 1-29 10 3 res Oil_cap_drive 1 0 130 100 1 0 0 [Feed_11]
# i j k idir type name ntime time skin WIFoil WIFgas WIFwater pres_bou temp_bou
Sw_bou So_bou Sg_bou
10 15 3 1 well 0.1 P10 1 0 0 1 1 1 130 100 0 1 0 [Feed_3 1]

```

```

9 15 3 1 well 0.1 P9 1 0 0 1 1 1 130 100 0 1 0 [Feed_3 1]
8 15 3 1 well 0.1 P8 1 0 0 1 1 1 130 100 0 1 0 [Feed_3 1]
7 15 3 1 well 0.1 P7 1 0 0 1 1 1 130 100 0 1 0 [Feed_3 1]
6 15 3 1 well 0.1 P6 1 0 0 1 1 1 130 100 0 1 0 [Feed_3 1]
5 15 3 1 well 0.1 P5 1 0 0 1 1 1 130 100 0 1 0 [Feed_3 1]
4 15 3 1 well 0.1 P4 1 0 0 1 1 1 130 100 0 1 0 [Feed_3 1]
3 15 3 1 well 0.1 P3 1 0 0 1 1 1 130 100 0 1 0 [Feed_3 1]
2 15 3 1 well 0.1 P2 1 0 0 1 1 1 130 100 0 1 0 [Feed_3 1]
1 15 3 1 well 0.1 P1 1 0 0 1 1 1 130 100 0 1 0 [Feed_3 1]

```

**\*INITIAL\_CONDITIONS**

```

# Feed
feed const [Feed_3 1]/

```

manual

```

# Saturations
# -----
sw const 0
so const 1
sg const 0

```

```

# Pressures
# -----
Po const 130

```

```

# Temperatures
# -----
T const 100

```

**\*TEMPERATURE off**

**\*INTEGRATION**

```

# tstart tstop
0 0

# dtmin dtmax dtstart dtfac cffac
100 3600 0.01 10 1

```

implicit Linsolver

**\*WELL\_COUPLING\_LEVEL**

4

**\*OUTPUT**

```

# cof_time cof_rate
1 1

```

```

# ntplot
10
P10
P9
P8
P7
P6
P5
P4
P3
P2
P1

```

```

Dt_Trend
0 3600 /

```

```

Dt_Prof
0 3600 /

```

```

screen_info 1

```

**\*END**



## Appendix 3: Relative permeability data

$S_w$	$K_{rw}$
0.1	0
0.11	0.003
0.12	0.005
0.15	0.013
0.2	0.025
0.25	0.038
0.3	0.05
0.35	0.082
0.4	0.114
0.45	0.145
0.5	0.177
0.55	0.233
0.6	0.289
0.65	0.344
0.7	0.4
0.75	0.48
0.8	0.56
0.85	0.64
0.9	0.72
0.95	0.86
1	1

$S_o$	$K_{ro}$
0.1	0
0.11	0.003
0.12	0.005
0.15	0.013
0.2	0.025
0.25	0.038
0.3	0.05
0.35	0.082
0.4	0.114
0.45	0.145
0.5	0.177
0.55	0.233
0.6	0.289
0.65	0.344
0.7	0.4
0.75	0.48
0.8	0.56
0.85	0.64
0.9	0.72
0.95	0.86
1	1

$S_g$	$K_{rg}$
0.1	0
0.11	0.003
0.12	0.005
0.15	0.013
0.2	0.025
0.25	0.038
0.3	0.05
0.35	0.082
0.4	0.114
0.45	0.145
0.5	0.177
0.55	0.233
0.6	0.289
0.65	0.344
0.7	0.4
0.75	0.48
0.8	0.56
0.85	0.64
0.9	0.72
0.95	0.86
1	1

# Appendix 4: Well/wellbore model in OLGA with AICV

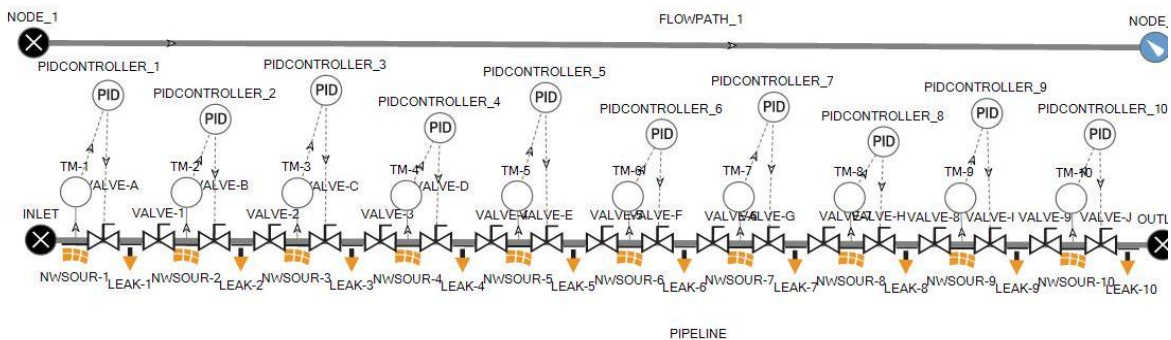
## 1. Introduction

<b>Project</b>	OLGA
<b>Case description</b>	Blackoil case
<b>Date</b>	
<b>Author</b>	SPT Group

## 2. Simulation Options

<b>Overall setting</b>	Flow model	OLGA
	Mass eq scheme	1STORDER
	Compositional model	BLACKOIL
	Debug	OFF
	Drilling	
	Phase	THREE
	Elastic walls	OFF
	Void in slug	SINTEF
	Steady state	OFF
	User defined plug-in	OFF
	Temp. calc.	WALL
	Wax deposition	
	Restart	OFF
	<b>Integration</b>	Simulation starttime
Simulation stoptime		300 d
Minimum time step		100 s
Maximum time step		3600 s

## 3. System Layout - Graphics



## 4. System Layout - Table

### 4.1 Summary

#### 4.1.1 Overall

No. of Branches	No. of Pipes	No. of Sections
2	2	60

#### 4.1.2 Flows

Branches	No. of Pipes	No. of Sections	Min. Section Length	At	Max. Section Length	At
PIPELINE	1	20	49.6 M	PIPE-1	49.6 M	PIPE-1
FLOWPATH_1	1	20	49.6 M	PIPE-1	49.6 M	PIPE-1

#### 4.2 Layout

Pipe no.	Branch	Label	Diameter	Roughness	XEnd	YEND	Wall
1 - 1	PIPELINE	PIPE-1	0.1 M	2.8E-05 M	992 M	0 M	WALL-1
2 - 1	FLOWPATH_1	PIPE-1	0.1 M	0.045 M	992 M	0 M	WALL-1

### 5. Insulation and Walls

#### 5.1 Material

Label	Density	Conductivity	Heat Capacity
MATER-1	7850 kg/m <sup>3</sup>	50 W/m-C	500 J/kg-C
MATER-2	2500 kg/m <sup>3</sup>	1 W/m-C	880 J/kg-C

#### 5.2 Walls

Label	Material	Wall thickness	Elastic
WALL-1	MATER-1	0.009 m	
	MATER-2	0.02 m	
	MATER-2	0.02 m	
WALL-2	MATER-1	0.0075 m	
	MATER-2	0.02 m	
	MATER-2	0.02 m	

### 6. Boundary Conditions

#### 6.1 Nodes

Label	Type	Pressure	Temperature
INLET	CLOSED		
OUTLET	CLOSED	50 bara	22 C
NODE_1	CLOSED		
NODE_2	PRESSURE	120 bara	100 C

#### 6.2 Heattransfer

Branch	Pipe	Interpolation	Houteroption.	Hambient	Tambient
PIPELINE	PIPE-1	SECTIONWISE	HGIVEN	1E-06 W/M2-C	100 C
FLOWPATH_1	PIPE-1	SECTIONWISE	AIR	1E-06 W/m2-C	100 C

### 6.3 Initial Conditions

Branch	Pipe	Mass Flow	VoidFraction
PIPELINE	PIPE-1	0	0 -
FLOWPATH_1	PIPE-1	0	0 -

## 7. Equipment

### 7.1 Valves

Label	Branch	Pipe	Section	Diameter	Opening	CD
VALVE-A	PIPELINE	PIPE-1	2	20 mm	1	0.84
VALVE-B	PIPELINE	PIPE-1	4	20 mm	1	0.84
VALVE-C	PIPELINE	PIPE-1	6	20 mm	1	0.84
VALVE-D	PIPELINE	PIPE-1	8	20 mm	1	0.84
VALVE-E	PIPELINE	PIPE-1	10	20 mm	1	0.84
VALVE-F	PIPELINE	PIPE-1	12	20 mm	1	0.84
VALVE-G	PIPELINE	PIPE-1	14	20 mm	1	0.84
VALVE-H	PIPELINE	PIPE-1	16	20 mm	1	0.84
VALVE-I	PIPELINE	PIPE-1	18	20 mm	1	0.84
VALVE-J	PIPELINE	PIPE-1	20	20 mm	1	0.84
VALVE-1	PIPELINE	PIPE-1	3	0.1 m	0	0.84
VALVE-2	PIPELINE	PIPE-1	5	0.1 m	0	0.84
VALVE-3	PIPELINE	PIPE-1	7	0.1 m	0	0.84
VALVE-4	PIPELINE	PIPE-1	9	0.1 m	0	0.84
VALVE-5	PIPELINE	PIPE-1	11	0.1 m	0	0.84
VALVE-6	PIPELINE	PIPE-1	13	0.1 m	0	0.84
VALVE-7	PIPELINE	PIPE-1	15	0.1 m	0	0.84
VALVE-8	PIPELINE	PIPE-1	17	0.1 m	0	0.84
VALVE-9	PIPELINE	PIPE-1	19	0.1 m	0	0.84

## 7. 2 Position

Label	Branch	Pipe	Section
POS-1	FLOWPATH_1	PIPE-1	1
POS-2	FLOWPATH_1	PIPE-1	2
POS-3	FLOWPATH_1	PIPE-1	3
POS-4	FLOWPATH_1	PIPE-1	4
POS-5	FLOWPATH_1	PIPE-1	5
POS-6	FLOWPATH_1	PIPE-1	6
POS-7	FLOWPATH_1	PIPE-1	7
POS-8	FLOWPATH_1	PIPE-1	8
POS-9	FLOWPATH_1	PIPE-1	9
POS-10	FLOWPATH_1	PIPE-1	10
POS-11	FLOWPATH_1	PIPE-1	11
POS-12	FLOWPATH_1	PIPE-1	12
POS-13	FLOWPATH_1	PIPE-1	13
POS-14	FLOWPATH_1	PIPE-1	14
POS-15	FLOWPATH_1	PIPE-1	15
POS-16	FLOWPATH_1	PIPE-1	16
POS-17	FLOWPATH_1	PIPE-1	17
POS-18	FLOWPATH_1	PIPE-1	18
POS-19	FLOWPATH_1	PIPE-1	19
POS-20	FLOWPATH_1	PIPE-1	20

# Appendix 5: Well/wellbore model in OPGA with ICD

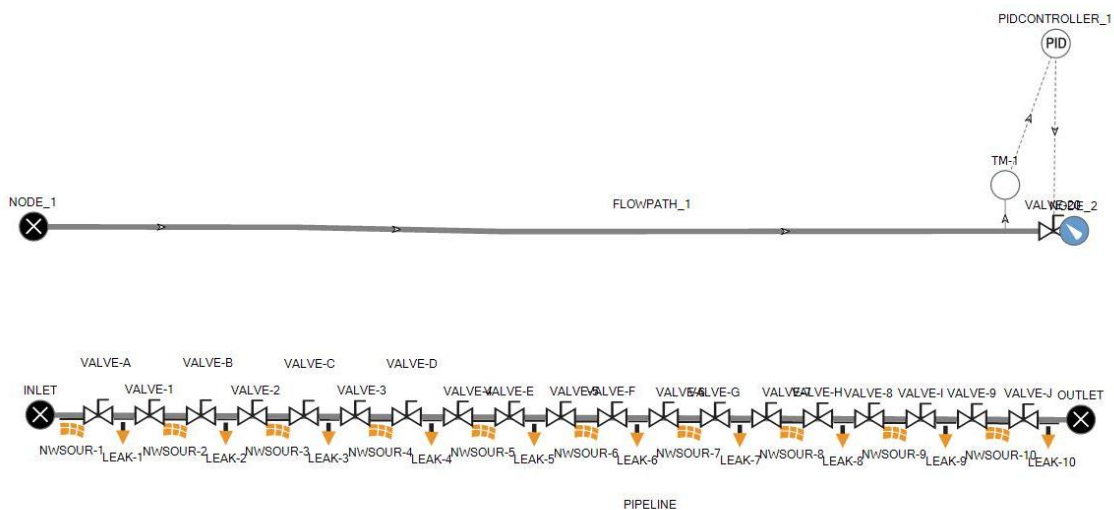
## 1. Introduction

<b>Project</b>	OLGA
<b>Case description</b>	Blackoil case
<b>Date</b>	
<b>Author</b>	SPT Group

## 2. Simulation Options

<b>Overall setting</b>	Flow model	OLGA
	Mass eq scheme	1STORDER
	Compositional model	BLACKOIL
	Debug	OFF
	Drilling	
	Phase	THREE
	Elastic walls	OFF
	Void in slug	SINTEF
	Steady state	OFF
	User defined plug-in	OFF
	Temp. calc.	WALL
	Wax deposition	
	Restart	OFF
	<b>Integration</b>	Simulation starttime
	Simulation stoptime	300 d
	Minimum time step	100 s
	Maximum time step	3600 s

## 3. System Layout - Graphics



## 4. System Layout - Table

### 4.1 Summary

#### 4.1.1 Overall

No. of Branches	No. of Pipes	No. of Sections
2	2	62

#### 4.1.2 Flows

Branches	No. of Pipes	No. of Sections	Min. Section Length	At	Max. Section Length	At
PIPELINE	1	20	49.6 M	PIPE-1	49.6 M	PIPE-1
FLOWPATH_1	1	21	49.59999999999999 M	PIPE-1	49.6 M	PIPE-1

### 4.2 Layout

Pipe no.	Branch	Label	Diameter	Roughness	XEnd	YEND	Wall
1 - 1	PIPELINE	PIPE-1	0.1 M	2.8E-05 M	992 M	0 M	WALL-1
2 - 1	FLOWPATH_1	PIPE-1	0.1 M	0.045 M	1041.6 M	0 M	WALL-1

## 5. Insulation and Walls

### 5.1 Material

Label	Density	Conductivity	Heat Capacity
MATER-1	7850 kg/m <sup>3</sup>	50 W/m-C	500 J/kg-C
MATER-2	2500 kg/m <sup>3</sup>	1 W/m-C	880 J/kg-C

### 5.2 Walls

Label	Material	Wall thickness	Elastic
WALL-1	MATER-1	0.009 m	
	MATER-2	0.02 m	
	MATER-2	0.02 m	
WALL-2	MATER-1	0.0075 m	
	MATER-2	0.02 m	
	MATER-2	0.02 m	

## 6. Boundary Conditions

### 6.1 Nodes

Label	Type	Pressure	Temperature
INLET	CLOSED		
OUTLET	CLOSED	50 bara	22 C
NODE_1	CLOSED		

NODE\_2 PRESSURE 120 bara 100 C

## 6. 2 Heattransfer

Branch	Pipe	Interpolation	Houteroption.	Hambient	Tambient
PIPELINE	PIPE-1	SECTIONWISE	HGIVEN	1E-06 W/M2-C	100 C
FLOWPATH_1	PIPE-1	SECTIONWISE	AIR	1E-06 W/m2-C	100 C

## 6. 3 Initial Conditions

Branch	Pipe	Mass Flow	VoidFraction
PIPELINE	PIPE-1	0	0 -
FLOWPATH_1	PIPE-1	0	0 -

## 7. Equipment

### 7. 1 Valves

Label	Branch	Pipe	Section	Diameter	Opening	CD
VALVE-A	PIPELINE	PIPE-1	2	20 mm	1	0.84
VALVE-B	PIPELINE	PIPE-1	4	20 mm	1	0.84
VALVE-C	PIPELINE	PIPE-1	6	20 mm	1	0.84
VALVE-D	PIPELINE	PIPE-1	8	20 mm	1	0.84
VALVE-E	PIPELINE	PIPE-1	10	20 mm	1	0.84
VALVE-F	PIPELINE	PIPE-1	12	20 mm	1	0.84
VALVE-G	PIPELINE	PIPE-1	14	20 mm	1	0.84
VALVE-H	PIPELINE	PIPE-1	16	20 mm	1	0.84
VALVE-I	PIPELINE	PIPE-1	18	20 mm	1	0.84
VALVE-J	PIPELINE	PIPE-1	20	20 mm	1	0.84
VALVE-1	PIPELINE	PIPE-1	3	0.1 m	0	0.84
VALVE-2	PIPELINE	PIPE-1	5	0.1 m	0	0.84
VALVE-3	PIPELINE	PIPE-1	7	0.1 m	0	0.84
VALVE-4	PIPELINE	PIPE-1	9	0.1 m	0	0.84
VALVE-5	PIPELINE	PIPE-1	11	0.1 m	0	0.84
VALVE-6	PIPELINE	PIPE-1	13	0.1 m	0	0.84
VALVE-7	PIPELINE	PIPE-1	15	0.1 m	0	0.84
VALVE-8	PIPELINE	PIPE-1	17	0.1 m	0	0.84
VALVE-9	PIPELINE	PIPE-1	19	0.1 m	0	0.84
VALVE-20	FLOWPATH_1	PIPE-1	22	0.075 m	1	0.84



## 7. 2 Position

Label	Branch	Pipe	Section
POS-1	FLOWPATH_1	PIPE-1	1
POS-2	FLOWPATH_1	PIPE-1	2
POS-3	FLOWPATH_1	PIPE-1	3
POS-4	FLOWPATH_1	PIPE-1	4
POS-5	FLOWPATH_1	PIPE-1	5
POS-6	FLOWPATH_1	PIPE-1	6
POS-7	FLOWPATH_1	PIPE-1	7
POS-8	FLOWPATH_1	PIPE-1	8
POS-9	FLOWPATH_1	PIPE-1	9
POS-10	FLOWPATH_1	PIPE-1	10
POS-11	FLOWPATH_1	PIPE-1	11
POS-12	FLOWPATH_1	PIPE-1	12
POS-13	FLOWPATH_1	PIPE-1	13
POS-14	FLOWPATH_1	PIPE-1	14
POS-15	FLOWPATH_1	PIPE-1	15
POS-16	FLOWPATH_1	PIPE-1	16
POS-17	FLOWPATH_1	PIPE-1	17
POS-18	FLOWPATH_1	PIPE-1	18
POS-19	FLOWPATH_1	PIPE-1	19
POS-20	FLOWPATH_1	PIPE-1	20
POS-21	FLOWPATH_1	PIPE-1	21

# Appendix 6: Numerical model calculation

## Volume of the wellbore

Radius of the equivalent wellbore tube is calculated from (5.16)

$$r_{we} = \sqrt{0.1^2 - 0.09^2}$$
$$r_{we} = 0.0436m$$

Then the volume of the wellbore can be calculated as,

$$V_{wellbore} = \pi(0.0436)^2(12.4) = 0.074m^3$$

## Gas inflow when AICV is opened

By applying the relevant parameters from table to (5.9),

$$q_g = \frac{\pi(0.1Da)(0.01)^2(1240cm)^2}{4 \cdot 0.0157cp} \cdot \frac{(120-110) \cdot 0.9869atm}{(300-10)cm}$$
$$q_g = 26.103 \frac{cm^3}{s} = 2.26 \frac{m^3}{d} = 0.094 \frac{m^3}{hr}$$

## Oil inflow when AICV is closed

From (3.5)

$$l_{ani} = \sqrt{\frac{1000}{100}} = 3.16$$

As  $\frac{L}{2} = 20.341ft < 118.11 = 0.9r_{eH}$  from (3.6)

$$a = \frac{40.682}{2} \left\{ 0.5 + \left[ 0.25 + \left( \frac{131.234}{40.682/2} \right)^4 \right]^{0.5} \right\}$$
$$a = 132.02ft$$

By applying these equations to (3.4)

$$q_o =$$

$$\frac{(1000mDa)(39.37ft)(1740.453-1595.415)psi}{141.2(1.1)(50) \left( \ln \left\{ \frac{\left[ 132.02 + \sqrt{132.02^2 - \left( \frac{40.682}{2} \right)^2} \right]}{40.682t/2} \right\} + \left( \frac{(3.16)(39.37)}{40.682} \right) \ln \left\{ \frac{(3.16)(39.37)}{0.328(3.16+1)} \right\} \right)}$$

$$q_o = 44.949 \frac{STB}{d} = 7.147 \frac{m^3}{d} = 0.298 \frac{m^3}{hr}$$

According to **Figure 5-3**, for a pressure drop of 10 bar, maximum flow through AICV is 3000 liters/hr. From the calculations it is seen that oil inflow is much less than this value. Therefore oil outflow is taken as 0.298 m<sup>3</sup>/hr when the AICV is opened.

#### Time taken to close the valve

Time taken to close the valve is calculated from time where the first gas bubble entered the wellbore. From (5.17), time taken to close the valve can be calculated as follows,

$$t_{close} = \frac{\pi(0.0436m)^2(12.4m)}{0.094m^3/hr}$$

$$t_{close} = 0.788hr$$

#### Oil inflow when AICV is closed

From (5.11), oil inflow when the AICV is closed, can be calculated as follows,

$$q_{oi,c} = \frac{0.298}{2} \cdot \frac{(3-0.1) \cdot 920 \cdot 9.81}{(10^6)}$$

$$q_{oi,c} = 3.9 \cdot 10^{-3} \frac{m^3}{hr}$$

#### Gas inflow when AICV is closed

From (5.10), oil inflow when the AICV is closed, can be calculated as follows,

$$q_{gi,c} = 0.094 \cdot \frac{(3-0.1) \cdot 65.63 \cdot 9.81}{(10^6)}$$

$$q_{gi,c} = 1.755 \cdot 10^{-4} \frac{m^3}{hr}$$

#### Oil outflow when AICV is closed

As shown in (5.14), oil outflow when AICV is closed, can be considered as 1% of the initial oil inflow and it can be calculated as,

$$q_{o\_out,c} = \frac{0.298}{100}$$

$$q_{o\_out,c} = 2.98 \cdot 10^{-3} \frac{m^3}{hr}$$

#### Gas outflow when AICV is closed

By applying (5.15), gas outflow can be calculated as,

$$q_{g\_out,c} = 3.9 \cdot 10^{-3} - 2.98 \cdot 10^{-3} + 0.175 \cdot 10^{-3}$$

$$q_{g\_out,c} = 1.095 \cdot 10^{-3} \frac{m^3}{hr}$$

#### Time taken to reopen the AICV

Based on the results obtained in **Error! Reference source not found.**, time taken to reopen the AICV can be calculated by the relationship obtained in (5.18). If it is considered that the AICV will be reopened, when the wellbore is completely filled with oil, time taken for that can be calculated as follows,

$$t_{reopen} = \frac{(1)0.0716}{1.095 \cdot 10^{-3} - 0.175 \cdot 10^{-3}}$$

$$t_{reopen} = 80.45hr = 3.3 \text{ days}$$

Based on this simple model it can be estimated that it takes 3.3 days to reopen the valve when the gas breakthrough occurs.

# References

- [1] V. Mathiesen, "Autonomous gas/water shut-off in field with gas/water breakthrough," in *SPE Aberdeen Summit Series Seminar*, ed: Society Of Petroleum Engineers Aberdeen Section, 2013.
- [2] R. F. Meyer and E. D. Attanasi, "Heavy oil and natural bitumen-strategic petroleum resources," *World*, vol. 434, p. 650.7, 2003.
- [3] A. Hart, "A review of technologies for transporting heavy crude oil and bitumen via pipelines," *Journal of Petroleum Exploration and Production Technology*, pp. 1-10, 2013/10/22 2013.
- [4] S. D. Joshi, "Cost/benefits of horizontal wells," in *SPE Western Regional/AAPG Pacific Section Joint Meeting*, 2003.
- [5] P. Fernandes, Z. Li, and D. Zhu, "Understanding the roles of inflow-control devices in optimizing horizontal-well performance," in *SPE Annual Technical Conference and Exhibition*, 2009.
- [6] F. T. Al-Khelaiwi, V. M. Birchenko, M. R. Konopczynski, and D. Davies, "Advanced Wells: A Comprehensive Approach to the Selection Between Passive and Active Inflow-Control Completions," *SPE Production & Operations*, vol. 25, pp. 305-326, 2010.
- [7] M. Halvorsen, G. Elseth, and O. M. Nævdal, "Increased oil production at Troll by autonomous inflow control with RCP valves," in *SPE Annual Technical Conference and Exhibition*, 2012.
- [8] H. A. Vidar Mathiesen, "Increased oil recovery of an old well, recompleted with Autonomous Inflow Control Valve (AICV)," in *ADIPEC 2013 Technical Conference*, Abu Dhabi, United Arab Emirates, 2013.
- [9] B. Hu, J. Sagen, G. Chupin, T. Haugset, A. Ek, and T. Sommersel, "Integrated Wellbore-Reservoir Dynamic Simulation," in *Asia Pacific Oil and Gas Conference and Exhibition*, 2007.
- [10] B. Hu, "A Transient Wellbore/Reservoir Flow Model," in *Drilling & well*, ed: Society of Petroleum Engineers, Bergen section, 2008.
- [11] D. E. Hembling, G. M. Berberian, A. A. Al-Mumen, S. Simonian, and G. Salerno, "Production Optimization of Multilateral Wells Using Passive Inflow Control Devices," *SAUDI ARAMCO JOURNAL OF TECHNOLOGY*, p. 3, 2010.
- [12] R. A. F. S. Moghaddam, H. Aakre, B. M. Halvorsen, "Near well simulations of heavy oil production with ICD completion," *Computational Methods in Multiphase Flow VII*, vol. 79, pp. 499-509, 2013.
- [13] M. J. Economides, A. D. Hill, and C. Ehlig-Economides, "Petroleum production systems," 1994.
- [14] J. J. Velarde, "Correlation of black oil properties at pressures below the bubble-point " Master of Science, Texas A&M University, 1996.
- [15] L. P. Dake, *Fundamentals of reservoir engineering*: Elsevier, 1983.
- [16] D. W. Peaceman, *Fundamentals of numerical reservoir simulation*: Elsevier, 2000.